conditions for the criterion established above. Thus $\mathcal{F}$ is indeed given by a multivalued first integral, i.e. $w = \sum_{j=1}^{m} \lambda_j \frac{df_j}{f_j}$. A further argument, still using the fact that the limit set of the holonomy is discrete, allows us to reduce m to 2, i.e. there are meromorphic maps Φ, Ψ on $\mathbf{C}^2$ such that $w = \frac{d\Phi}{\Phi} + \lambda \frac{d\Psi}{\Psi}$. Thus $F = (\Phi, \Psi)$, and so $\mathcal{L}$ is defined by the form $\frac{dx}{x} + \lambda \frac{dy}{y} = 0$. This finishes the proof.

References

[1] Camacho, C., Lins Neto, A., Sad, P., Foliations with algebraic limit set, *Ann. of Math.* **136** (1992), 429–446.

[2] Camacho, C., Sad, P., Invariant varieties through singularities of holomorphic vector fields, *Ann. of Math.* **115** (1982), 579–595.

[3] Jouanolou, J.P., *Équations de Pfaff algébriques*, Lecture Notes in Math. **708**, Springer-Verlag, Berlin-Heidelberg-New York 1979.

[4] Lehman, D., Résidus de sous-variétés invariantes d'un feuilletage singulier, *Ann. Inst. Fourier* **41** (1991), 211–258.

[5] Lins Neto, A., Algebraic solutions of polynomial differential equations and foliations in dimension two, in: *Holomorphic Dynamics* (X. Gomez-Mont et al., eds.), Lecture Notes in Math. **1345**, Springer-Verlag, Berlin-Heidelberg-New York 1986, 192–232.

[6] Siu, Y., *Techniques of Extension of Analytic Objects*, Marcel Dekker, New York 1974.

Techniques in the Theory of Local Bifurcations: Blow-Up, Normal Forms, Nilpotent Bifurcations, Singular Perturbations

Freddy DUMORTIER

Notes written with the assistance of Bert SMITS

Limburgs Universitair Centrum
Universitaire Campus
B-3590 Diepenbeek
Belgium

Abstract

We present a number of results mostly obtained in the last years and only published recently or even not yet published. We do not give complete proofs but emphasize the different techniques and the precise way they have to be used. These notes are meant to be a helpful guide in struggling through the different research papers they are based on.

The material is presented in five chapters and three appendices.

Chapter 1 : Blowing up singularities of vector fields
Chapter 2 : Normal forms, unfoldings of nilpotent singularities and the Bogdanov-Takens bifurcation
Chapter 3 : Rescalings and Liénard equations in unfoldings of nilpotent singularities of codimension 3
Chapter 4 : Blow-up of families in the study of the nilpotent focus of codimension 3
Chapter 5 : Singular perturbations and the "canard" phenomenon.

1 Blowing up singularities of vector fields

For the sake of completeness and in view of its importance, we present here quite extensively this by now well-known technique in the study of singularities of vector fields; we restrict ourselves to C^∞ vector fields.

1.1 Polar blow up and related directional blow-up

Let X be a C^∞ vector field on $\mathbb{R}^n$ with a singularity at the origin, $X(0) = 0$. Consider the mapping

$$\phi : S^{n-1} \times \mathbb{R} \to \mathbb{R}^n : ((\bar{x}_1, \ldots, \bar{x}_n), r) \mapsto (r\bar{x}_1, \ldots, r\bar{x}_n)$$

D. Schlomiuk (ed.), Bifurcations and Periodic Orbits of Vector Fields, 19–73.

with $\sum_{i=1}^{n} \bar{x}_i^2 = 1$.

Then the pull-back $\hat{X}$, with $\phi_*(\hat{X}) = X$, is a C^∞-vector field on $S^{n-1} \times \mathbb{R}$ (i.e. $D\phi_p(\hat{X}(p)) = X \circ \phi(p)$, where $\hat{X}$ is the blown up vector field).

In $\mathbb{R}^2$, we parametrize S^1 by the angular coordinate θ and use

$$\phi : S^1 \times \mathbb{R} \to \mathbb{R}^2 : (\theta, r) \mapsto (r\cos\theta, r\sin\theta),$$

whence the name "polar". (One verifies that $j_k(X)(0) = 0$ implies $j_k(\hat{X})(u) = 0$, for all $u \in S^1 \times \{0\}$). This means that the degenerate singularity has been turned into a whole circle of singularities. On $S^1 \times \mathbb{R}_0^+$, ϕ is a diffeomorphism.

In practice, one simplifies the calculations by looking at charts and performing the so-called "directional" blow-ups.

$$\text{x-direction :} \quad (\bar{x}, \bar{y}) \mapsto (\bar{x}, \bar{y}\bar{x}) \tag{1}$$

$$\text{y-direction :} \quad (\bar{x}, \bar{y}) \mapsto (\bar{x}\bar{y}, \bar{y}) \tag{2}$$

E.g. on $\{x \neq 0\} = \{\theta \neq \frac{\pi}{2}; \frac{3\pi}{2}\}$, (1.1) is the same as polar blow up, up to the analytic coordinate change $(\theta, r) \mapsto (r\cos\theta,\ \mathrm{tg}\,\theta)$. Indeed, $(r\cos\theta,\ \mathrm{tg}\,\theta \cdot r\cos\theta) = (r\cos\theta, r\sin\theta)$.

The "pull-backs" of the directional blow-up maps are hence merely expressions of $\hat{X}$ in well chosen coordinate systems. Here the degenerate singularity is turned into a line of singularities.

After blowing up the singularity to a circle one can "desingularize" $\hat{X}$ by considering $\bar{X} = 1/r^k \hat{X}$, k being the order of the largest zero jet of X at 0, i.e. $j_l(X)(0) = 0$ if $\ell \leq k$; $j_{k+1}(X)(0) \neq 0$. For the directional blow-up we use $1/\bar{x}^k \hat{X}$ resp. $1/\bar{y}^k \hat{X}$.

These last vector fields are no longer coordinate expressions of $\bar{X}$, but are equal to $\bar{X}$ up to an analytic coordinate change and multiplication with a positive analytic function. This positive factor does not constitute any problem since we are only concerned with the orbit structure (phase portrait) of X around the singularity (a precise definition of the equivalences we want to use will be given below). It could matter if we would have the intention to keep track of the time on the orbits, but even here — as we will see — the construction remains interesting.

A typical example where one (polar) blow-up suffices to obtain the phase portrait near a singularity is given by the vector fields in Example 1.

Example 1 Let $X_a = (ax^2 - 2xy)\frac{\partial}{\partial x} + (y^2 - axy)\frac{\partial}{\partial y} + 0(\|(x,y)\|^3)$, $a > 0$.

The phase portrait of $\bar{X}_a$ near $r = 0$ is given by the left picture in Figure 1. The singularities on $\{r = 0\}$ are hyperbolic saddles. In the right picture of Figure 1 the phase portrait of X_a is shown.

1.2 C^0-equivalence and C^0-conjugacy

We now formalize an equivalence relation describing the behaviour of a dynamical system in the neighbourhood of a singularity.

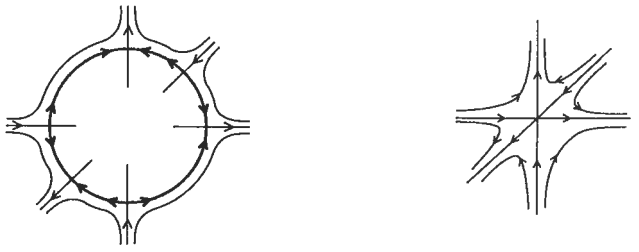

$\bar{X}_a$ (on $S^1 \times \mathbb{R}^+$) X_a (on $\mathbb{R}^2$)

Figure 1 : A singularity and its polar blow-up

Definition Two vector fields X (at p) and Y (at q) are called *locally C^0-equivalent* if there exists a homeomorphism h from a neighbourhood V of p onto a neighbourhood W of q such that h sends orbits $X|V$ to orbits $Y|W$ preserving their sense, i.e. for any $x \in V$ and $t \in \mathbb{R}$ such that $X_{[0,t]}(x) \subset V$, there exists $t' \in \mathbb{R}$ with $t \cdot t' > 0$ and $h(X_{[0,t]}(x)) = Y_{[0,t']}(h(x))$.

A stronger property is local C^0-conjugacy :

Definition X (at p) and Y (at q) are called *locally C^0-conjugate* if there exists a homeomorphism h from a neighbourhood V of p onto a neighbourhood W of q such that for all $t \in \mathbb{R} : h \circ X_t = Y_t \circ h$ whenever both sides remain in the respective neighbourhoods. Here X_t denotes the (local) flow of X.

In Example 1, using the (polar) blow-up, one can show that X_a and $X_{a'}$ are locally C^0-conjugate for any $a, a' > 0$ (see [D] or [CD]).

Furthermore, $j_2(X_a)(0)$, the 2-jet of X_a at 0, is C^0-determining (for C^0-conjugacy), in the sense that any vector field with the same 2-jet is C^0-conjugate to it.

If in the previous definition we change "homeomorphism" to "C^r-diffeomorphism", then we speak about a local C^r-equivalence, resp. a local C^r-conjugacy. These stronger notions will be used whenever possible.

1.3 Successive blowing up

One can think of examples of vector fields with singularities where one blowing up will not suffice to determine their topological type.

Example 2 Let $Y_{a,b} = y\frac{\partial}{\partial x} + (ax^2 + bxy)\frac{\partial}{\partial y} + O(\|(x,y)\|^3)$, $a \neq 0$. We require three steps to "desingularize" it (see below for a precise definition of desingularization) and identify it topologically as a "cusp" :

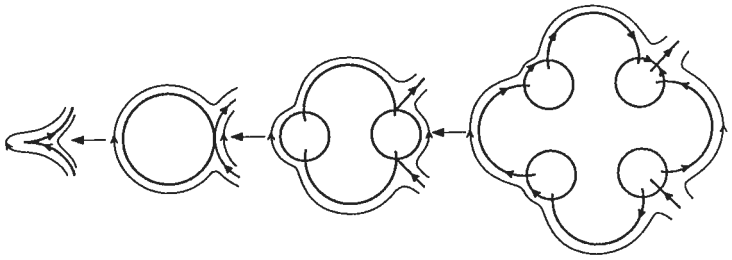

Figure 2 : Successive blow-ups of the cusp singularity

In the sequel, singularities of vector fields on $\mathbb{R}^2$, with a 1-jet linearly conjugate to $y\frac{\partial}{\partial x}$ will be called "nilpotent". Moreover, if they are C^0-conjugate to the phase portrait in Figure 2, we call them cusps.

In $\mathbb{R}^2$, the procedure of successive blow-up can be formalized as follows : we use

$$\tilde{\phi} : \{z; ||z|| > \frac{1}{2}\} \subset \mathbb{R}^2 \to \mathbb{R}^2 : z \mapsto z - \frac{z}{||z||}$$

and then divide out by a power of $(||z|| - 1)$. To blow up a second time in a point z_0 on the unit circle we translate it to the origin and apply again $\tilde{\phi}$; the second blow-up mapping is therefore

$$\phi_2 = T_{z_0} \circ \tilde{\phi} \ ,$$

where

$$T_{z_0}(z) = z + z_0 \ .$$

After a sequence of n blow-ups $\phi_1 \circ \ldots \circ \phi_n$ (including the required divisions) we find a C^∞ vector field $\bar{X}^n$ defined one some open domain $U_n \subset \mathbb{R}^2$.

Let $\Gamma_n = (\phi_1 \circ \ldots \circ \phi_n)^{-1}(0) \subset U_n$, and denote by A_n the connected component of $\mathbb{R}^2 \backslash \Gamma_n$ with a non-compact closure. One verifies that $\partial A_n \subset \Gamma_n$; it is homeomorphic to S^1 and it consists of a finite number of regular C^∞-arcs meeting transversely at the endpoints. The effect of the divisions is seen as follows : there exists an analytic function $F_n > 0$ on A_n with $\hat{X}^n = F_n \bar{X}^n$ and $\hat{X}^n | A_n$ is analytically conjugate to $X | \mathbb{R}^2 \backslash \{0\}$ by means of $(\phi_1 \circ \ldots \circ \phi_n) | A_n$.

A natural question to ask is whether this process will decrease the complexity of the singularities, and whether eventually we will get some desingularization (only "simple" singularities) in a finite number of steps. Explaining the answer given in [D1], requires the following notion :

Definition A vector field X on $\mathbb{R}^n$ with $X(0) = 0$ satisfies a *Lojasiewicz inequality* if there exist $k \in \mathbf{N}_1$ and $c > 0$ such that

$$||X(x)|| \geq c||x||^k \quad \text{for all } x \in U \ ,$$

where U is some neighbourhood of 0.

This property is not as exceptional as it may seem : for instance, analytic vector fields always satisfy a Lojasiewicz inequality at an isolated singularity. Furthermore, any k-jet X^k has some extension X^ℓ $(\ell \geq k)$ satisfying the condition.

Theorem *If X satisfies a Lojasiewicz inequality, then there exists a finite sequence of blow-ups $\phi_1 \circ \ldots \circ \phi_n$ leading to a vector field $\bar{X}^n$ along ∂A_n such that the singularities of $\bar{X}^n$ on ∂A_n are*

(a) *isolated singularities p at which $\bar{X}^n$ is hyperbolic or semi-hyperbolic, with the property that $j_\infty(\bar{X}^n | N^c)(p) \neq 0$ if N^c is a center manifold for $\bar{X}^n$ at p;*

(b) *regular smooth closed (with boundary) curves (or possible ∂A_n as a whole in the case $n = 1$) along which $\bar{X}^n$ is normally hyperbolic.*

Moreover, the position and the properties of the singularities mentioned above only depend on a finite jet of X.

Remark Such as $\bar{X}^n$ having on ∂A_n only singularities as described in (a) and (b) is what we call a desingularization (or a nice decomposition) of X at 0. We also say that X (satisfying a Lojasiewicz inequality at 0) can be desingularized after a finite number of (polar) blow-ups.

In fact one can prove that the Lojasiewicz property at 0 is equivalent to the existence of a desingularization after a finite number of blow-ups (see [D1]).

1.4 Quasi-homogeneous blow-up

The method of successive (polar) blow-up is interesting for the study of singularities in general. In many cases, however, we can significantly speed up the procedure. Let us only consider an example where the "quasi-homogeneous part of lowest degree" is "determining". For general information on the method we refer tot [BM] and [Br].

Definition A function $f : \mathbb{R}^n \to \mathbb{R}$ is called *quasi-homogeneous of type* $(\alpha_1, \ldots, \alpha_n) \in \mathbf{N}^n$ and degree k if for any $r \in \mathbb{R}$:

$$f(r^{\alpha_1} x_1, \ldots, r^{\alpha_n} x_n) = r^k f(x_1, \ldots, x_n).$$

A vector field $X = \sum_{j=1}^{n} f_j(x_1, \ldots, x_n) \frac{\partial}{\partial x_j}$ is called *quasi-homogeneous of type* $(\alpha_1, \ldots, \alpha_n)$ and degree $k+1$ if f_j is quasi-homogeneous of type $(\alpha_1, \ldots, \alpha_n)$ and degree $k + \alpha_j$, for all j.

Examples $(ax^2 - 2xy)\dfrac{\partial}{\partial x} + (y^2 - axy)\dfrac{\partial}{\partial y}$ is homogeneous of degree 2, hence quasi-homogeneous of type (1,1) and degree 2.

$y\dfrac{\partial}{\partial x} + ax^2\dfrac{\partial}{\partial y}$ is quasi-homogeneous of type (2,3) and degree 2.

In the spirit of Section 1.1 we formalize a quasi-homogeneous blow-up procedure. Let

$$\varphi : S^{n-1} \times \mathbb{R} \to \mathbb{R}^n : ((\bar{x}_1, \ldots, \bar{x}_n), r) \mapsto (r^{\alpha_1}\bar{x}_1, \ldots, r^{\alpha_n}\bar{x}_n)$$

with $\sum_{i=1}^{n} \bar{x}_i^2 = 1$. To see the impact of the method in a simple way, we work on the vector field $Y_{a,b}$ from Example 2.

The appropriate quasi-homogeneous blow-up is :

$$\varphi : S^1 \times \mathbb{R} \to \mathbb{R}^2 : (\theta, r) \mapsto (r^2\cos\theta, r^3\sin\theta)$$

or, preferably the related directional blow-ups :

x-direction : $\begin{cases} x = r^2 \\ y = r^3\bar{y} \end{cases}$ and also $\begin{cases} x = -r^2 \\ y = r^3\bar{y} \end{cases}$,

y-direction : $\begin{cases} x = r^2\bar{x} \\ y = r^3 \end{cases}$.

In contrast to what we did with ("homogeneous") polar blow-ups we now need to consider two blow-ups in the x-direction ($x < 0$ and $x > 0$), since we use an even exponent for r. One blow up would only cover $\{x \neq 0\}$ in the case of an odd exponent.

After substituting and dividing by r we obtain respectively the vector fields

$$\begin{cases} \dot{r} = \frac{1}{2}r\bar{y} \\ \dot{\bar{y}} = a - \frac{3}{2}\bar{y}^2 \end{cases} \qquad \begin{cases} \dot{r} = -\frac{1}{2}r\bar{y} \\ \dot{\bar{y}} = a + \frac{3}{2}\bar{y}^2 \end{cases} \qquad \begin{cases} \dot{r} = \frac{a}{3}r\bar{x}^2 \\ \dot{\bar{x}} = 1 - \frac{2}{3}a\bar{x}^3 \end{cases}.$$

The complete picture (in $((\bar{x}, \bar{y}), r)$-coordinates) is given by Figure 3. Since all the singularities are hyperbolic, we have a complete desingularization after one blow-up.

To end this section, let us mention the following result about the determination of jets. It has been proved in [Bru] that a quasi-homogeneous component is C^0-determining when it has the origin as an isolated singularity not being a center.

1.5 Quasi-homogeneous components and Newton's diagram

To detect determining quasi-homogeneous components there is the possibility of using Newton's diagram.

The best way to define and also to memorize Newton's diagram is to work with the dual 1-form of the given vector field.

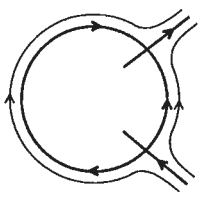

Figure 3 : A desingularized cusp

For a vector field $X_1\dfrac{\partial}{\partial x} + X_2\dfrac{\partial}{\partial y}$, its dual 1-form is the 1-form $\omega = i_X\Omega$, with $\Omega = dx \wedge dy$; i.e.,

$$\omega = X_1 dy - X_2 dx .$$

Take now

$$j_\infty\omega(0) = \sum_{\substack{i,j \geq 0 \\ i+j \geq 1}} a_{ij}x^i y^j dx + \sum_{\substack{i,j \geq 0 \\ i+j \geq 1}} b_{ij}x^i y^j dy .$$

The support of ω (or X) is defined to be

$$S : \{(i+1, j) | a_{ij} \neq 0\} \cup \{i, j+1) | b_{ij} \neq 0\} .$$

The Newton polyhedron of ω or X is the convex hull Γ of the set

$$P = \bigcup_{(r,s) \in S} \{(r, s) + \mathbb{R}^2_+\},$$

while the Newton diagram of ω or X is the union γ of the compact faces γ_k of Γ. We obtain a quasi-homogeneous component by restricting $(i+1, j)$ and $(i, j+1)$ to some γ_k.

Newton's diagram of the vector field $Y_{a,b}$ from Example 2 has one compact face, related to the quasi-homogeneous component

$$y\frac{\partial}{\partial x} + ax^2\frac{\partial}{\partial y} .$$

This component clearly has an isolated singularity at 0 without being a center.

2 Normal forms, unfoldings of nilpotent singularities, and the Bogdanov-Takens bifurcation

We now briefly present a normal form procedure for both vector fields and families of vector fields and apply it to unfoldings of nilpotent singularities. We also present a study of the generic Bogdanov-Takens bifurcation.

2.1 Normal forms for vector fields

Let the vector field X be given by a linear part A and a C^∞-function f, which satisfies $f(0) = 0$, $Df(0) = 0$. The aim of normal form theory is to determine for each given linear field A a restricted class of non-linearities $\mathcal{F}_n$ as small and as simple as possible, and such that for each f, the equation can be brought into the form

$$X' = A + \tilde{f}, \quad \text{with} \quad \tilde{f} \in \mathcal{F}_n$$

by a suitable C^∞-coordinate change. To this purpose, we consider the adjoint linear action on $\chi^\infty(\mathbb{R}^n)$, the space of germs of C^∞ vector fields at 0 :

$$ad_A : \chi^\infty(\mathbb{R}^n) \to \chi^\infty(\mathbb{R}^n) : X \mapsto [A, X] = DX(A) - AX \ .$$

The restriction of this operator to $H^m(\mathbb{R}^n)$, the space of homogeneous polynomial vector fields of degree m, will be denoted by $ad_m A$. Let $B^m = Im\ ad_m A$ and G^m some complement, i.e. $B^m \oplus G^m = H^m(\mathbb{R}^n)$. The main theorem of this section was proved by F. Takens in 1974. We also refer to [GH] for a slightly different proof.

Theorem [T] *Let X be a C^r vector field, defined in a neighbourhood of 0 with $X(0) = 0$ and $DX(0) = A$; $r \in \mathbb{N}_1$. Let B^k and G^k be as above. Then there is an analytic change of coordinates $\phi : (\mathbb{R}^n, 0) \to (\mathbb{R}^n, 0)$ in the neighbourhood of 0 such that $X' = \phi_*(X)$ is of the form*

$$X'(y) = Ay + g_2(y) + g_3(y) + \ldots + g_r(y) + O(\| y \|^{r+1})$$

with $g_i \in G^i$, for all $i \in \{2, \ldots, r\}$.

From a computational point of view, the normal form theory presented in this way is not yet satisfactory. Improvements concern the choice of the complementary spaces. In fact, one can always use $G^m = Ker(ad_m A^T)$, where A^T denotes the transpose of A (see [V]).

To see this, we just have to define an inner product $\langle , \rangle_m$ on $H^m(\mathbb{R}^n)$ in which

$$\langle (ad_m A^T)g, h\rangle_m = \langle g, (ad_m A)h\rangle_m, \forall g, h \in H^m(\mathbb{R}^n).$$

Then, for this inner product, we have

$$(ad_m A^T) = (ad_m A)^T$$

hence

$$H^m(\mathbb{R}^n) = Im(ad_m A) \oplus Ker(ad_m A^T).$$

The inner product is defined by

$$\langle \sum_{|\sigma|=m} a_\sigma x^\sigma, \sum_{|\sigma|=m} b_\sigma x^\sigma \rangle_m := \sum_{|\sigma|=m} \sigma! \langle a_\sigma, b_\sigma \rangle$$

for any $a_\sigma, b_\sigma \in \mathbb{R}^m$ with $|\sigma| = m$.

2.2 Normal forms for families of vector fields

Here the technique is similar. The main difference is that the adjoint action of $A = DX_0(0)$ must now also be considered at the 0-jet level, because, in a family, the origin need not be kept singular.

We therefore consider the action $ad_k A$ on $\bar{J}^m_k$, the space of k-jets of vector fields on $\mathbb{R}^m$ (they need not be 0 at the origin).

$\bar{B}^k$ is again defined as $Im(ad_k A)$, and $\bar{G}^k$ is some complementary subspace. This generalization is also due to Takens [T3].

Theorem *Let X be a C^∞ p-parameter family of vector fields on $\mathbb{R}^m$ (defined in a neighbourhood of 0), then for $k, \ell \in \mathbb{N}_1$ there exists an analytic diffeomorphism $\phi : \mathbb{R}^p \times \mathbb{R}^n \to \mathbb{R}^p \times \mathbb{R}^n$ with $\pi \circ \phi = \pi$ (π is the projection on the parameter space) such that the l-jet of $\phi_*(X) = \tilde{X}$ has the form*

$$j_\ell(\tilde{X})(0) = j_\ell(X_0)(0) + \sum \lambda_1^{i_1} \ldots \lambda_p^{i_p} Z_{i_1,\ldots,i_p} + O((\| \lambda \| + \| x \|)^{k+1}),$$

where all $Z_{i_1,\ldots,i_p} \in \bar{G}^k$, and where the sum takes place over all indices $i_1, \ldots, i_p \geq 0$ with $1 \leq \sum_j i_j \leq \ell$.

Corollary If, for fixed k and $\ell = k$, $\{X_1, \ldots, X_r\}$ denotes a basis of $\bar{G}^k$, then the theorem implies that the family X is analytically conjugate respecting the parameter (i.e. for a conjugacy $(x, \lambda) \mapsto (\varphi_\lambda(x), \lambda)$) to

$$A + \sum_{i=1}^{r} f_i(\lambda) X_i + O((\| \lambda \| + \| x \|)^{k+1}),$$

where $f_i(\lambda)$ are polynomials in λ of degree $\leq k$.

2.3 Applications to unfoldings of nilpotent singularities

As an example, we describe a normal form procedure for unfoldings of singularities in $\mathbb{R}^2$ having a nilpotent 1-jet, i.e. the linear part is conjugate to $y\frac{\partial}{\partial x}$. We proceed as in Section 1.

Step 1 *Calculation of $Ker(ad_m A^T)$.*
A straightforward calculation gives

$$Ker(ad_m A^T) = \{\alpha x^m \frac{\partial}{\partial y} + \beta(y x^{m-1} \frac{\partial}{\partial y} + x^m \frac{\partial}{\partial x}) | \alpha, \beta \in \mathbb{R}\}$$

Step 2 *Good choice of G^m, $m \geq 1$.*
As

$$[y\frac{\partial}{\partial x}, x^m \frac{\partial}{\partial y}] = m y x^{m-1} \frac{\partial}{\partial y} - x^m \frac{\partial}{\partial y} \in Im(ad_m A)$$

it follows that $yx^{m-1}\frac{\partial}{\partial y} \notin Im(ad_m A)$. $Im(ad_m A)$ has codimension 2, so we can take G^m to be

$$G^m = \{\alpha x^m \frac{\partial}{\partial y} + \beta x^{m-1} y \frac{\partial}{\partial y} | \alpha, \beta \in \mathbb{R}\}.$$

Step 3 *Choice of G°.*
At the zero level, the complement is spanned by $\frac{\partial}{\partial y}$, since $[y\frac{\partial}{\partial x}, \frac{\partial}{\partial x}] = 0$ and $[y\frac{\partial}{\partial x}, \frac{\partial}{\partial y}] = -\frac{\partial}{\partial x}$.

Consider now a C^∞-unfolding of the nilpotent singularity, i.e., a family X_λ with X_0 having a nilpotent singularity at the origin. For any large enough N it is C^∞-conjugate (respecting the parameter) to some

$$y\frac{\partial}{\partial x} + [F(x,\lambda) + yG(x,\lambda)]\frac{\partial}{\partial y} + Q_1\frac{\partial}{\partial x} + Q_2\frac{\partial}{\partial y},$$

where $Q_i = O((\| x, y) \| + \| \lambda \|)^N)$, and where F, G are polynomials of degree N.

Performing the λ-dependent coordinate change $Y = y + Q_1$, $X = x$, we obtain the system

$$\begin{cases} \dot{X} = Y \\ \dot{Y} = F(X,\lambda) + YG(X,\lambda) + Q_2'(X,Y,\lambda); \end{cases}$$

hence we may suppose (up to C^∞-conjugacy, respecting the parameter) to work with

$$y\frac{\partial}{\partial x} + [F(x,\lambda) + yG(x,\lambda) + Q(x,y,\lambda)]\frac{\partial}{\partial y}$$

which, after a development of Q in powers of y, becomes

$$y\frac{\partial}{\partial x} + [F(x,\lambda) + yG(x,y) + y^2Q(x,y,\lambda)]\frac{\partial}{\partial y}$$

with $Q = O((\| (x,y) \| + \| \lambda \|)^N)$; F and G are perhaps no longer polynomial, but are at least C^∞ and satisfy $F(0,0) = \frac{\partial F}{\partial x}(0,0) = G(0,0) = 0$.

For further use (in Section 4) we assume the generic condition $(\frac{\partial^2 F}{\partial x^2}(0,0))\cdot(\frac{\partial G}{\partial x}(0,0)) \neq 0$. By this we will be able to reduce $F(x,0)$ to x^2 and $F(x,\lambda)$ to a fold-catastrophe.

Step 4 *Reduction of $F(x,0)$ to x^2.*
For this operation it is better to work with the dual 1 form $\omega_\lambda = y\,dy - [F(x,\lambda) + yG(x,\lambda) + y^2Q(x,y,\lambda)]dx$.

We can write $F(x,0)dx = d(\bar{F}(x,0))$, and since $\frac{\partial^2 F}{\partial x^2}(0,0) \neq 0$, we can find a local C^∞-diffeomorphism $X = u(x)$, $u(0) = 0$, such that $\bar{F}(x,0) = X^3/3$, hence $F(x,0)dx = X^2dX$.

Simultaneously, we take $Y = \pm y$, depending on whether $\frac{\partial u}{\partial x}(0) > 0$ or < 0.

A normal form, obtained in this way is no longer C^∞-conjugate but C^∞-equivalent, respecting the parameter, to the original expression, since we also allow multiplication by a positive function (the coordinate change does not respect the form $\Omega = dx \wedge dy$).

Step 5 *Reduction of $F(x,\lambda)$ to a fold-catastrophe.*
By the preparation theorem of Malgrange (Mather's version : see e.g. [Brö]) there exists a C^∞-map $\mu(\lambda)$ and a family of C^∞ diffeomorphisms $U_\lambda(x) = x + G(x^2) + O(\| \lambda \|)$ with

$$U_\lambda^*(F(x,\lambda)dx) = (x^2 + \mu(\lambda))dx; \quad \mu(0) = 0.$$

The original family X_λ becomes so C^∞-equivalent, respecting the parameter, to

$$y\frac{\partial}{\partial x} + (x^2 + \mu(\lambda) + y\bar{G}(x,\lambda) + y^2\bar{Q}(x,y,\lambda))\frac{\partial}{\partial y},$$

and after performing and extra linear coordinate change we get

$$y\frac{\partial}{\partial x} + (x^2 + \mu(\lambda) + y(\nu(\lambda) \pm x + x^2h(x,\lambda)) + y^2Q(x,y,\lambda))\frac{\partial}{\partial y},$$

where all functions are C^∞ and $Q = O((\| (x,y) \| + \| \lambda \|)^N)$.

2.4 The Bogdanov-Takens bifurcation

In the case $\lambda \in \mathbb{R}^2$ and $\lambda \mapsto (\mu(\lambda), \nu(\lambda))$ is of maximal rank at 0 (hence a local diffeomorphism), we call the family, given at the end of Section 2.3, a generic Bogdanov-Takens bifurcation. Bogdanov ([B]) proved that all generic B.T. bifurcations are locally weakly C^0-equivalent to the so-called quadratic (or standard) one, given by

$$y\frac{\partial}{\partial x} + (x^2 + \mu + y(\nu \pm xy))\frac{\partial}{\partial y}.$$

The bifurcation diagram (for the + case) up to C^∞-diffeomorphism is (as in Figure 4) given by the ν-axis and two curves L and H tangent to it. The ν-axis, outside the origin, represents (generic) saddle-node bifurcations, H represents (codimension 1) Hopf bifurcations and L represents generic loop-bifurcations. Both H and L can be written as graphs of C^∞-functions resp. $\mu = \alpha(\nu)$ and $\mu = \beta(\nu)$ for $\nu < 0$ with $\alpha(\nu) = -\nu^2 + O(\nu^2)$ and $\beta(\nu) = -49\nu^2/25 + O(\nu^2)$.

By weak C^0-equivalence between X_λ and Y_η we mean the existence of neighbourhoods V and W of 0 in resp. phase space (x,y) and parameter space λ, and a family of homeomorphisms h_λ, for $\lambda \in W$, all defined on a fixed V and being a C^0-equivalence on V between X_λ and $Y_{\eta(\lambda)}$.

If moreover $(x,y,\lambda) \mapsto (h_\lambda(x,y), \eta(\lambda))$ depends continuously on λ, then we drop the prefix "weak" and speak about a C^0-equivalence for families.

For the generic Bogdanov-Takens bifurcation it has been proved (see [DR]) that there is always a local C^0-equivalence with the quadratic one.

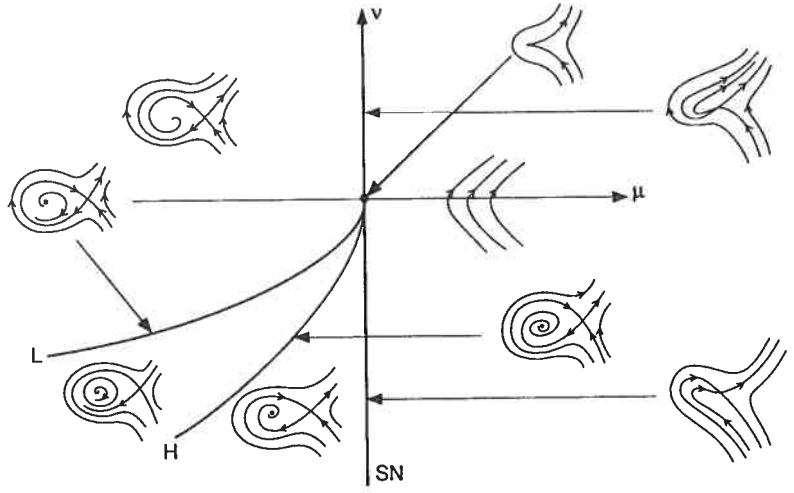

Figure 4 : The Bogdanov-Takens bifurcation diagram

However, in the sequel, when studying more complicated nilpotent bifurcations, we will not pay attention to this technical problem and only consider weak C^0-equivalence.

Let us also mention that the quadratic B.T. bifurcation can be studied completely, i.e. for all $(\mu,\nu) \in \mathbb{R}^2$ and $(x,y) \in \mathbb{R}^2$ (see [DRc]). The global bifurcation diagram (including the different global phase portraits) is similar to the local one (see Figure 4) with $H = \{(-\nu^2,\nu)|\nu < 0\}$ and $L : \{(\beta(\nu),\nu)|\nu < 0\}$.

2.5 More about normal forms and unfoldings of nilpotent singularities: codimension 3

We consider generic 3-parameter families unfolding a nilpotent singularity of codimension 3. In this case $\frac{\partial G}{\partial x}(0,0) = 0$. One can show that X_0 is C^∞-equivalent to a germ of a vector field having as 4-jet

$$y\frac{\partial}{\partial x} + (x^2 + \beta x^3 y)\frac{\partial}{\partial y}$$

for some value of β. In order to have a cusp singularity of codimension 3, whose generic unfoldings are stable, we add the generic condition $\beta \neq 0$. Up to a linear change of coordinates we have

$$j_4(X_0(0)) = y\frac{\partial}{\partial x} + (x^2 \pm x^3 y)\frac{\partial}{\partial y}\ .$$

By means of a C^∞-equivalence (C^∞-dependence on λ) one can change the family X_λ into the following normal form

$$y\frac{\partial}{\partial x} + (x^2 + \mu(\lambda) + yK(y,\lambda)G(x,\lambda) + y^2Q(x,y,\lambda))\frac{\partial}{\partial y}$$

with $K(0,\lambda) = 1$, and

$$G(x,\lambda) = \nu_0(\lambda) + \nu_1(\lambda)x + \alpha(\lambda)x^2 + \beta(\lambda)x^3 + O(x^4)$$

with $\beta(0) = \pm 1$, $\nu_0(0) = \nu_1(0) = \alpha(0) = 0$.

The genericity of the family amounts to saying that locally (μ,ν_0,ν_1) can be chosen as new independent parameters.

We are now ready to prove that all these bifurcations are locally weakly C^0-equivalent to the model unfolding

$$y\frac{\partial}{\partial x} + (x^2 + \mu + y(\nu_0 + \nu_1 x \pm x^3))\frac{\partial}{\partial y}\ .$$

The way to study these families and others is by trying to describe the bifurcation set and a related stratification of the parameter space in order to

(a) have only one type of stratification up to C^∞-diffeomorphism or at least up to homeomorphism; and

(b) have in all strata exactly one phase portrait (up to C^0-equivalence) not depending on the specific family.

The bifurcation diagram reveals a cone-like structure with the origin as vertex and the interaction with a sphere as shown in Figure 5. In this bifurcation, but also in the other ones of codimension 3, that we will describe in Chapter 3, the bifurcation set and the stratification referred to in point (a) above, are only determined up to homeomorphism, while the homeomorphisms in point (b) are not known to depend continuously on the parameter (we only have weak C^0-equivalence at the family-level).

It is interesting to remark that this is the first known example of a "non-algebraic" local bifurcation diagram. Indeed there appears a flat contact between two lines C and L at the point C_2. Together with [DF] (see also appendix 3) where is given a three parameter family of quadratic vector fields representing a generic unfolding of a cusp of codimension 3, this provides a negative answer to a question of Coppel (see [C1]), asking whether it is possible to characterize phase portraits of quadratic vector fields in the plane by means of polynomial equations.

It is not even possible to do this with analytic equations. The same example shows that the closure of the set of limit cycles for quadratic vector fields in the plane cannot be a semi-analytic set. That this can make the study of limit cycles quite complicated will be seen in the lectures by R. Roussarie [R] as well as in other sections of these proceedings (e.g. Local Dynamics and Nonlocal Bifurcations (Yu. Ilyashenko)).

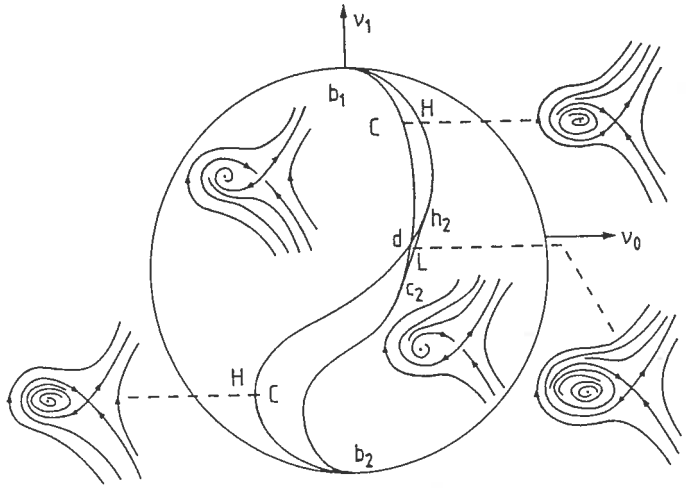

Figure 5 : Bifurcation diagram of the generic codimension 3-cusp

3 Rescalings and Liénard equations in unfoldings of nilpotent singularities of codimension 3

By a nilpotent singularity of codimension 3 in this chapter we mean a vector field in $\mathbb{R}^2$ with nilpotent 1-jet and 4-jet C^∞ conjugate to

$$y\frac{\partial}{\partial x} + (\varepsilon_1 x^3 + dx^4 + bxy + ax^2y + ex^3y)\frac{\partial}{\partial y} \qquad b > 0, \varepsilon_1 = \pm 1 \ .$$

If we assume in addition that $b \neq 2\sqrt{2}$ (when $\varepsilon_1 = -1$) and $5\varepsilon_1 a - 3bd \neq 0$ we have a 4-jet C^∞-equivalent to

$$y\frac{\partial}{\partial x} + (\varepsilon_1 x^3 + bxy + \varepsilon_2 x^2 y + fx^3 y)\frac{\partial}{\partial y}$$

with $b > 0$, $\varepsilon_i = \pm 1$, and $b \neq 2\sqrt{2}$ for $\varepsilon_1 = -1$.

By means of a quasi-homogeneous blow-up we can desingularize the vector fields locally and find the following phase portraits We now want to study the families X_λ unfolding such a singularity, i.e., X_0 has such a singularity at 0.

Similarly as in the preceding chapter, we can put X_λ into the following normal form for C^∞-equivalence :

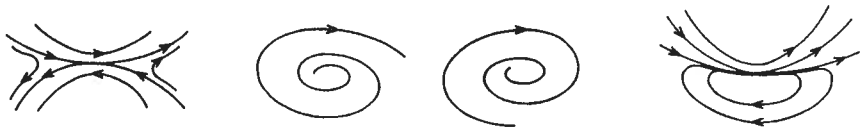

saddle type ($\varepsilon_1 = 1$) | focus type ($\varepsilon_1 = -1, 0 < b < 2\sqrt{2}$) | elliptic type ($\varepsilon_1 = -1, b > 2\sqrt{2}$)

Figure 6 : Some nilpotent singularities of codimension 3

$$y\frac{\partial}{\partial x} + (\varepsilon_1 x^3 + \mu_2 x + \mu_1 + y(\nu + b(\mu_1, \mu_2, \nu)x + \varepsilon_2 x^2 + x^3 h(x, \mu_1, \mu_2, \nu)) + y^2 Q(x, y, \mu_1, \mu_2, \nu))\frac{\partial}{\partial y}$$

with $\varepsilon_i = \pm 1$, b, h, Q all C^∞, $b(0) = b > 0$, $Q = O(||(x, y, \mu_1, \mu_2, \nu)||^N)$ for some a priori given N. In fact ν, μ_1, μ_2 represent C^∞ functions in λ. However we will restrict the study to 3-parameter generic unfoldings so that we can take (ν, μ_1, μ_2) as (new) independent parameters. Furthermore, up to the time reversing coordinate change $(x, y, \mu_1, \mu_2, \nu, t) \mapsto (-x, y, -\mu_1, \mu_2, -\nu, -t)$ we may take $\varepsilon_2 = +1$.

Of course the time reversal will transform attracting points and closed orbits into repelling ones, but since our aim is just to describe the bifurcation diagram and the different phase portraits, it suffices to treat the case $\varepsilon_2 = +1$.

We denote the above-mentioned families by (X_S, X_F, X_E), depending on the type of singularity they unfold (see Figure 6). We again intend to show that the "standard unfoldings"

$$y\frac{\partial}{\partial x} + (\varepsilon_1 x^3 + \mu_2 x + \mu_1 + y(\nu + bx + x^2))\frac{\partial}{\partial y}$$

are good models for weak C^0-equivalence. The study of these codimension 3-bifurcations turns out to be much more involved than the treatment of the previous cases.

A number of new techniques have to be introduced and one has to rely on results that were not commonly used in bifurcation theory before. In these notes we can of course not make a detailed technical elaboration but we will only present the main ingredients. For a complete treatment we will refer to the different papers on which the proof relies. The main source is [DRS2] presenting the conjectured bifurcation diagram (and different phase portraits) for all the cases and reducing the study to a number of precise subproblems.

For example, in the saddle case the problem is completely reduced to the study of certain (generalized) Liénard equations, and taking [DR2] into account this also works for the focus case. Probably the techniques of [DR2], which we will present below, can permit us to draw the same conclusion for the elliptic case as well.

For the treatment of the Liénard equations we can refer to [DRc] where the problems related to the saddle and to the elliptic case are completely solved, while in some Liénard equations related to the focus case it remains to be proved that they contain at most one limit cycle.

In the presentation of these results and techniques we will concentrate on the saddle and the focus and pay less attention to the elliptic case.

3.1 The saddle case ($\varepsilon_1 = 1$)

The singularities of X_S are given by

$$\begin{cases} y = 0 \\ x^3 + \mu_2 x + \mu_1 = 0 \ . \end{cases}$$

The discriminant condition on the second equation $27\mu_1^2 + 4\mu_2^3 = 0$ gives two lines along which we have non-simple singularities and hence candidates for saddle-node bifurcation and more degenerate ones.

We actually recover as bifurcation diagram the Riemann-Hugoniot catastrophe (or cusp catastrophe, see [Brö]), in (μ_1, μ_2)-plane, giving a surface in (ν, μ_1, μ_2)-space. We can also find a surface of candidates for Andronov-Hopf and more degenerate bifurcations by elimination of x between

$$\begin{cases} x^3 + \mu_2 x + \mu_1 = 0 \\ \nu + b(\mu_1, \mu_2, \nu)x + x^2 + x^3 h(x, \mu_1, \mu_2, \nu) = 0 \ . \end{cases}$$

Since $b(0) > 0$ we can use the implicit function theorem to show that the surface in (ν, μ_1, μ_2)-space is diffeomorphic to the one defined in (x, μ_1, μ_2)-space by $x^3 + \mu_2 x + \mu_1 = 0$, representing a cusp-catastrophe surface. Both surfaces — in (ν, μ_1, μ_2)-space — touch along a line whose asymptotics are given by $(\mu_1 \sim r^3, \mu_2 \sim r^2, \nu \sim r)$. Along this line we can expect generic Bogdanov-Takens bifurcations, but of course a proof is needed. As the surfaces are conic-like with respect to the origin we will often represent them by means of their intersection with a small sphere S^2.

For further investigation — with respect to the cone structure of the bifurcation diagram and the needed proofs — it is now better to use a common technique in the domain known as "rescaling".

The choice of the rescaling is based on the asymptotics of the line of possible B.T. bifurcations. It also respects the asymptotics of the conic structure of the two above-mentioned surfaces. We can hence expect to be able to study a number of phenomena in a "uniform way".

Later on, we will see that one rescaling will not suffice to finish the study. Let us call this first one the "principal rescaling". It is given by

$$\begin{cases} x = r\bar{x} \\ y = r^2\bar{y} \\ t = \bar{t}/r \end{cases} \qquad \begin{cases} \mu_1 = r^3\bar{\mu}_1 \\ \mu_2 = r^2\bar{\mu}_2 \\ \nu = r\bar{\nu} \end{cases}$$

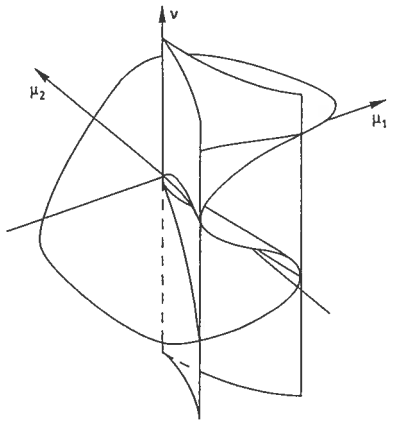

Figure 7 : Surfaces of double singularities and div 0-singularities

with $\bar{\mu}_1^2 + \bar{\mu}_2^2 + \bar{\nu}^2 = 1$. The rescaled vector field then becomes

$$\bar{X}_{\bar{\lambda}} = \bar{X}^P_{\bar{\lambda}} + O(r),$$

where

$$\bar{X}^P_{\bar{\lambda}} = \bar{y}\frac{\partial}{\partial \bar{x}} + (\bar{x}^3 + \bar{\mu}_2\bar{x} + \bar{\mu}_1 + \bar{y}(\bar{\nu} + b\bar{x}))\frac{\partial}{\partial \bar{y}} \ .$$

This $\bar{X}^P_{\bar{\lambda}}$ is the representative in the phase plane of the family of second order scalar differential equation

$$\ddot{x} = x^3 + \mu_2 x + \mu_1 + \dot{x}(\nu + bx)$$

which is a (generalized) cubic Liénard equation with linear damping, i.e., it is of the form $\ddot{x} = A(x) + B(x)\dot{x}$ with $A(x)$ cubic and $B(x) = \nu + bx$ linear.

In fact, all Liénard equations of this form can be reduced to the conditions $b > 0$ and $A(x) = \pm x^3 + \mu_2 x + \mu_1$ by an affine coordinate change in the phase plane.

The idea is now to study the Liénard equations first and then to determine the parts of the bifurcation diagram that persist after adding the remainder $O(r)$. Especially the phenomena described by transversality conditions will persist, because of the existing stability theorems of implicit-function type (transversality theory of Thom, see [H]). To apply these results we will have to limit our phase plane to some compact set $A \subset \mathbb{R}^2$ (which can be arbitrarily large and preferably is).

For a fixed value of b, the three-parameter family $\bar{X}^P_{\bar{\lambda}}$ remains invariant under the principal rescaling. $\bar{X}^P_{\bar{\lambda}}$ can be considered as the quasi-homogeneous part of lowest degree of X_λ. Along the curves in parameter space defined by $(\nu, \mu_1, \mu_2) = (r\bar{\nu}, r^3\bar{\mu}_1, r^2\bar{\mu}_2)$, for

$r > 0$, the phase portrait does not change. It therefore suffices to study it for λ on the sphere $\mu_1^2 + \mu_2^2 + \nu^2 = 1$ or on the cube $\max(c_1|\mu_1|, c_2|\mu_2|, c_3|\nu|) = 1$, for some $c_i > 0$.

We can now first make a study of the singularities of $\bar{X}_\lambda^P$, exactly in the same way as we did in the study of X_λ, before rescaling. We will find two surfaces, of double singularities and degenerate simple singularities, respectively, touching along a curve through the origin.

By taking $c_1 = c_2 = 1$ and $c_3 > 0$ sufficiently small, one can quite easily show that on the faces $\nu = 1/c_3$ and for (μ_1, μ_2) with $|\mu_1| \leq 1$ and $|\mu_2| \leq 1$ the bifurcation diagram and related phase portraits are limited to a semi-hyperbolic bifurcation of codimension 3 (see [BDST]), involving only singularities and no other interesting phenomena.

On the faces $\{\mu_2 = 1\}$, $\{\mu_1 = \pm 1\}$ and on $\{\mu_2 = -1\}$ for $|\mu_1| \geq 3/(2\sqrt{3})$, there are no bifurcations at all and the unique stable phase portrait is given by a single hyperbolic saddle point.

Hence all relevant phenomena occur when

$$\mu_2 = -1, \quad -\frac{2}{3\sqrt{3}} \leq \mu_1 \leq \frac{2}{3\sqrt{3}}, \quad -N \leq \nu \leq N$$

for some $N = 1/c_3$ sufficiently large.

By normal form calculation one can show that on $\{\mu_1 = -2/(3\sqrt{3})\}$ and on $\{\mu_1 = 2/(3\sqrt{3})\}$ only generic saddle-node bifurcations occur except for one point on each line, where we have a generic Bogdanov-Takens bifurcation. For $|\mu_1| < 2/(3\sqrt{3})$ all vector fields have three simple singularities, namely two hyperbolic saddles and between them an antisaddle. This last point is always a hyperbolic focus except along one line H connecting the two B.T.-points.

This line represents generic Hopf-bifurcations except for the point $\{\mu_1 = \nu = 0\}$, where we encounter a quite degenerate situation since the vector field $\bar{X}_\lambda^P$ with $\lambda = (0, 0, -1)$ is time-reversible and has a center at the origin.

All these local facts can be proven by normal form calculations at the respective singularities. Life gets more complicated when we try to investigate the global behaviour. However, the following simple observation turns out to be of a substantial help in the study of closed orbits and saddle connections, namely the rotational property with respect to the parameter ν. The family of vector fields depending on the parameter ν (for fixed values of μ_1 and μ_2) denoted by X_ν, is a family of rotated vector fields (Perko calls this a semi-complete family (mod $y \equiv 0$) of rotated vector fields, see [P]).

This means

(i) Singular points are independent of ν.

(ii) The derivative of the angle between X_0 and X_ν with respect to ν is strictly positive for $y \neq 0$.

(iii) $\tan\theta \to \pm\infty$ as $\nu \to +\infty$, where θ is the angle between the vector field and the positive x-axis.

Not all items in this definition are really important (especially not the third one), but as they are all satisfied here we can as well mention them.

This rotational property has a number of nice consequences, among which the following : any hyperbolic attracting (repelling) limit cycle expands (shrinks) monotonically as ν increases (see Figure 8), as a consequence of Poincaré-Bedixson's theorem. Moreover, if a

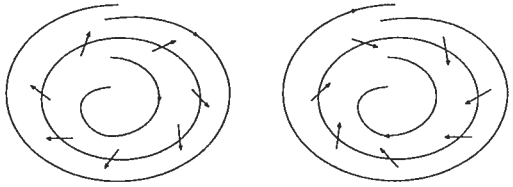

Figure 8 : Expansion (contraction) of a hyperbolic limit cycle

closed orbit of X_ν prasses through a point $p(\nu)$, then for all $\nu' \neq \nu$ no closed orbit of $X_{\nu'}$ can pass through $p(\nu)$.

The rotational property also implies that the separatrices of the two saddles move in a monotone way with non-zero velocity (with respect to ν). So, using the rotational property,

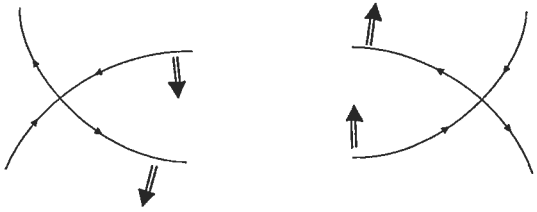

Figure 9 : Movement of the separatrices under the rotational property

it will follow that if any saddle connection occurs, it will occur generically and along a line $\nu = \nu(\mu_1)$ on $\{\mu_2 = -1\}$.

Let us come back to the line H, exactly in the middle, i.e., $m = (\nu, \mu_1, \mu_2) = (0, 0, -1)$, where we have

$$y\frac{\partial}{\partial x} + (x(x^2 - 1) + bxy)\frac{\partial}{\partial y}$$

This vector field is time-reversible under the mapping $(x, t) \mapsto (-x, -t)$, see Figure 10 for its phase portraits. The same rotational property makes it easier to show that outside this point the curve H represents generic (codimension 1) Andronov-Hopf bifurcations.

To the left of m we have a supercritical Hopf bifurcation with the creation of an attracting limit cycle for increasing ν, to the right a subcritical Hopf bifurcation with the

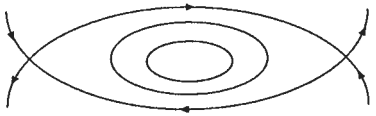

Figure 10 : Time reversible system $\bar{X}^P_{(0,0,-1)}$ in saddle case

disappearance of a repelling limit cycle for increasing ν. As long as the attracting limit cycle (created to the left of m) stays hyperbolic it will expand monotonically for increasing ν.

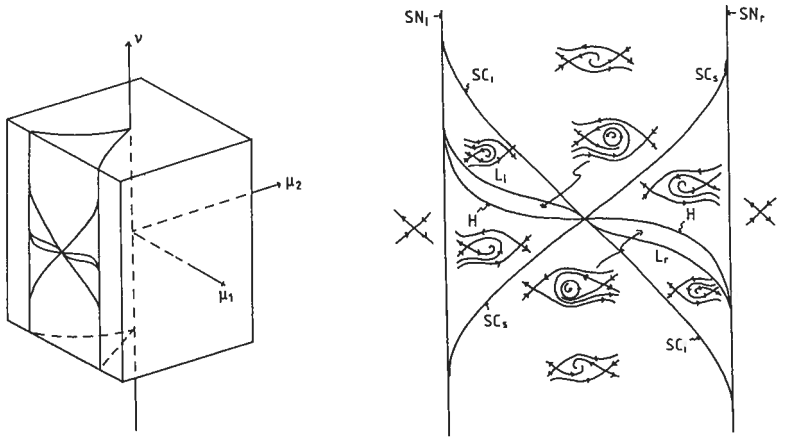

Figure 11 : Bifurcation diagram for the Liénard equation of saddle type

Of course — as we already observed — for ν sufficiently large this limit cycle can no longer be present. Indeed the line $D = \{x = -\nu/b\}$, representing the points of divergence zero, moves in a monotone way from right to left. On both sides of this line the divergence keeps its sign. Hence for ν sufficiently big, D lies left of all singularities inhibiting the possibility of having a closed orbit. As in the meantime the rotational property implies somewhere the presence of a generic loop bifurcation (generic homoclinic connection : see [ALGM] or [BDST]), it is quite natural to expect that the attracting cycle created at a generic Hopf bifurcation, expands monotonically until it disappears at a generic loop bifurcation.

Therefore, however, we need to be sure about the hyperbolicity of the limit cycle at each moment of its evolution. Fortunately, this is guaranteed by the following theorem of

Coppel.

Theorem (see [C2] and [DRc]) *Consider the system*

$$\begin{cases} \dot{x} = F(x) - y \\ \dot{y} = g(x) \end{cases}$$

with $F \in C^2$ and $g \in C^1$, defined for $x \in]\alpha, \beta[$ $(\alpha, \beta \in \bar{\mathbb{R}})$, satisfying the following conditions (i) – (iv) *and either* (v) *or* (vi) *:*

(i) *$f(x) = F'(x)$ has a unique zero $x_0 < 0$; $f(x) < 0$ (resp. > 0) as $\alpha < x < x_0$ (resp. $x_0 < x < \beta$);*

(ii) *$F(0) = 0$, $F(\xi_0) = 0$ for $\alpha < \xi_0 < x_0$;*

(iii) *$xg(x) > 0$ for $x \neq 0$, $x \in]\alpha, \beta[$;*

(iv) *the simultaneous equations*

$$F(x_1) = F(x_2), \lambda(x_1) = \lambda(x_2)$$

have at most one solution $x_1 < x_0 < 0 < x_2$, where $\lambda(x) = g(x)/f(x)$;

(v) *the function $F(x)f(x)/g(x)$ is decreasing for $\alpha < x < \xi_0$;*

(vi) *the function $F(x)f(x)/g(x)$ is increasing for $0 < x < \beta$ and $\lim_{x \to \alpha^+} F(x) \leq \lim_{x \to \beta^-} F(x)$.*

Then the equation has at most one periodic orbit in the region $x \in]\alpha, \beta[$. The periodic orbit is attracting and hyperbolic if it exists.

To apply the theorem, we have to change the Liénard equation into its "normal" expression by means of the so-called "Liénard transformation" $y \mapsto -y + F(x)$:

$$\begin{cases} \dot{x} = y \\ \dot{y} = -g(x) + yf(x) \end{cases} \Rightarrow \quad \begin{cases} \dot{x} = F(x) - y \\ \dot{y} = g(x) \, . \end{cases}$$

One can check that for the system under consideration, (i) – (iv) and (vi) are satisfied. Hence the limit cycles always remain hyperbolic.

The rest of the bifurcation diagram (heteroclinic and homoclinic connections) can now be completed by means of the rotational property with respect to ν, as well as some "semi-rotational" property with respect to μ_1 (rotational on the halfplanes $\{y > 0\}$ and $\{y < 0\}$.

We also use the symmetry $(x, y, \nu, \mu_1, \mu_2, t) \mapsto (-x, y, -\nu, -\mu_1, \mu_2, -t)$. Returning to the unfolding $\bar{X}_{\bar{\lambda}}$, we see that, by a transversality argument, all bifurcations and phase portraits persist when adding $O(r)$, except near the central point $(\bar{\nu}, \bar{\mu}_1, \bar{\mu}_2) = (0, 0, -1)$ on the face $\bar{\mu}_2 = -1$. To study $\bar{X}_{\bar{\lambda}}$ near this point we perform a blowing up in the parameter space $(\bar{\nu}, \bar{\mu}_1, r)$ (inducing the so called "central" rescaling) :

$$\begin{cases} \bar{x} = x' \\ \bar{y} = y' \end{cases} \qquad \begin{cases} \bar{\nu} = \tau\nu' \\ \bar{\mu}_1 = \tau\mu_1' \\ r = \tau v \end{cases}$$

with $\nu'^2 + \mu_1'^2 + v^2 = 1$. We thus obtain

$$X'_{\lambda'} = X^S + \tau(\mu'_1 + \nu' y' + v x'^2 y')\frac{\partial}{\partial y'} + O(\tau^2)$$

with

$$X^S = \bar{X}^P_{(0,0,-1)} = y'\frac{\partial}{\partial x'} + (x'^3 - x' + bx'y')\frac{\partial}{\partial y'} .$$

X^S is not a Hamiltonian vector field ($\mathrm{div}(X^S) = bx'$) but it does have an integrating factor K. Writing the dual 1-form of $X'_{\lambda'}$ as $\omega_{\lambda'}$ we have (for some K and H (see [DRS2] for precise expressions)) :

$$K\omega_{\lambda'} = dH - \tau K(\mu'_1 + \nu' y' + \nu x'^2 y')dx' + O(\tau^2) .$$

In order to obtain the complete bifurcation diagram we need to use some more machinery, such as the method of perturbation from a Hamiltonian vector field, estimating the related Abelian integrals, as has been done by H. Żołądek in [Z].

Unfortunately this analysis is only valid on the regular part of the Hamiltonian and near the center. Near the double heteroclinic connection we need to perform an extra study. The complete elaboration can be found in [DRS2] and we refer to appendix 1 for a short survey. After lengthy calculations we get the bifurcation diagram and related phase portraits as presented in Figure 12.

We see that near the line $(\bar{\nu}, \bar{\mu}_1, \bar{\mu}_2) = (0, 0, -r)$ the situation is more complicated than for the (limiting) Liénard-family: now there exists the possibility of having two limit cycles; this only occurs for parameter values in a tiny sector.

3.2 The focus case ($\varepsilon = -1; 0 < b < 2\sqrt{2}$)

Here we will try to imitate the "saddle programme" for as long as it works by detecting the singularities, applying the principal rescaling and performing the study of the related Liénard equations. The rotational properties hold as well as Coppel's theorem. Indeed, wherever there is but one singularity in the game the theorem applies. Hence the limit cycles surrounding only one singularity are hyperbolic. However, now there is the possibility of having limit cycles surrounding three singularities. Let us call them "large" limit cycles.

A modification of Coppel's theorem can be found in [DRc], but it does not work in general, and we are left with a conjecture. There is a proof that a large limit cycle can never surround a small one, but in a certain region of the parameter space (see Figure 13) one cannot yet prove that there is at most one large limit cycle. In [DRc] is conjectured that this is always the case.

In Figure 13 we show the bifurcation diagram and the stable phase portraits for the Liénard equations (in the phase plane) :

$$\bar{X}^P_{\bar{\lambda}} = \bar{y}\frac{\theta}{\partial \bar{x}} + (-\bar{x}^3 + \bar{\mu}_2\bar{x} + \bar{\mu}_1 + \bar{y}(\bar{\nu} + b\bar{x}))\frac{\partial}{\partial y} .$$

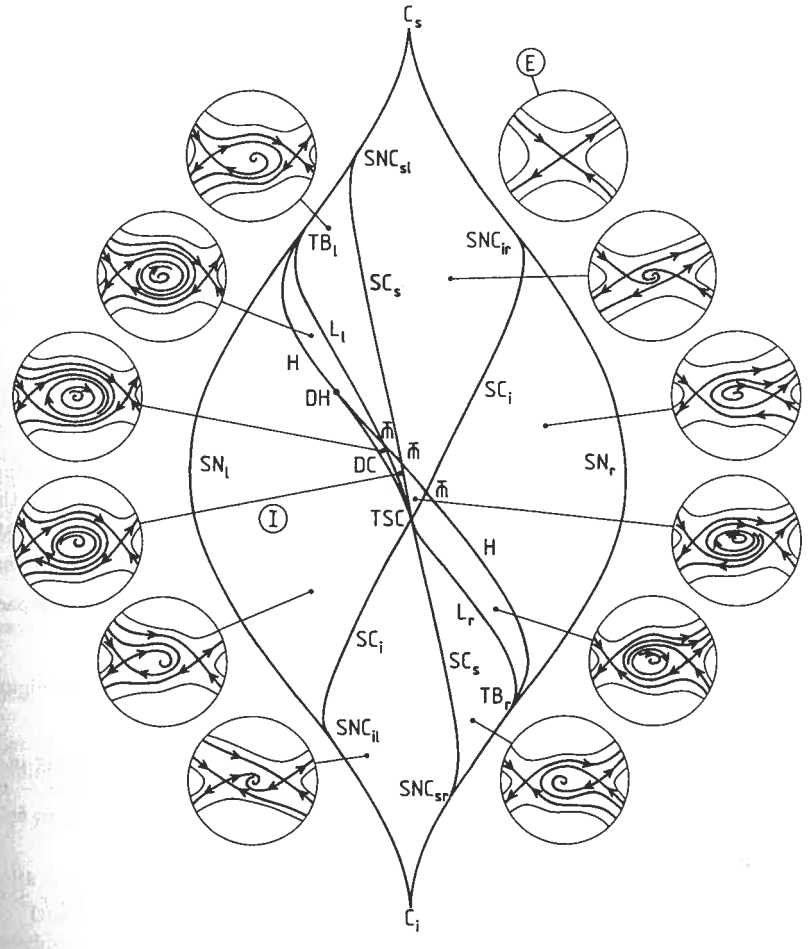

Figure 12 : Bifurcation diagram for the saddle case

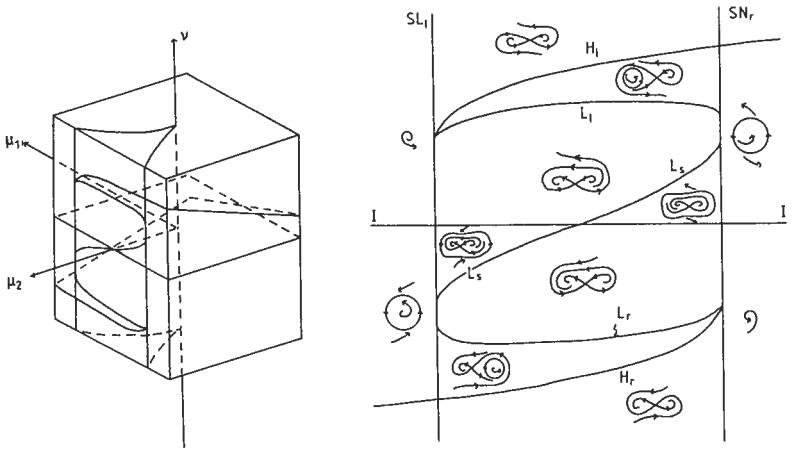

Figure 13 : Bifurcation diagram for the Liénard equations of focus type

The different faces of the cube are again defined by $\bar{\mu}_1 = \pm 1$, $\bar{\mu}_2 = \pm 1$ and $\bar{\nu} = \pm N$ for some large $N > 0$. The shaded area represents the region where the proof is not finished in the sense that multiple limit cycles are not yet excluded (there is also a symmetric counterpart under the symmetry $(\bar{x}, \bar{y}, \bar{\nu}, \bar{\mu}_1, \bar{\mu}_2, t) \mapsto (-\bar{x}, \bar{y}, -\bar{\nu}, -\bar{\mu}_1, \bar{\mu}_2, -t)$).

Again all phenomena for $\bar{X}^P_\lambda$ are described by transversality conditions on some compact domain in $(\bar{x}, \bar{y})$-space, except along the plane $\{\bar{\nu} = 0\}$:

(i) for $(\bar{\nu}, \bar{\mu}_1, \bar{\mu}_2) = (0, 0, \pm 1)$ we have the time-reversible systems represented in Figure 14 exhibiting an infinite number of closed orbits.

(ii) in all other values of $\{\bar{\nu} = 0\}$ on the cube we see a limit cycle (dis)appearing in a generic way at infinity in the $(\bar{x}, \bar{y})$-plane. (the genericity of the disappearance — or appearance — can be checked on the Poincaré-sphere related to the cubic vector field $\bar{X}^P_\lambda$ (see [DRc] for an account)).

So what are the Liénard equations going to teach us about $\bar{X}_{\bar{\lambda}} = \bar{X}^P_\lambda + O(r)$, for $r > 0$, near $\{\bar{\nu} = 0\}$?

We cannot expect — as in (ii) — to see a bifurcation "at infinity", but if we fix an arbitrary (large enough) compact set A in the $(\bar{x}, \bar{y})$-plane we can expect to see limit cycles moving through ∂A and going outside A (or coming inside A).

By making a "good" choice of ∂A this bifurcation at the boundary can be represented by a neat curve, as we do in Figure 15. We will however not go into details here, as the next paragraph will show us that this analysis is not necessary.

$\bar{X}^P_{(0,0,-1)}$ $\bar{X}^P_{(0,0,1)}$

Figure 14 : Time-reversible systems in focus case

Let us now look at point (i). To study $\bar{X}_{\bar{\lambda}}$ near the points $(\bar{\nu}, \bar{\mu}_1, \bar{\mu}_2) = (0, 0, \pm 1)$ we proceed as in the saddle case and perform exactly the same blowing up in parameter space (introducing the "central" rescaling) as we did there. Again the study is essentially reduced to a problem of perturbation from a Hamiltonian vector field after introducing an integrating factor. We refer to [DRS2] and especially to [Z] for the detailed elaboration.

Once more one sees limit cycles, simple and double ones this time, growing beyond any (a priori given) compact domain A in $(\bar{x}, \bar{y})$-plane. Let us also choose, without going into details, the boundary ∂A in such a way that this bifurcation at ∂A is given by a single curve. At this level the complete bifurcation diagram that we get for $\bar{X}_{\bar{\lambda}} = \bar{X}^P_\lambda + O(r)$, with $r > 0$ small and with $(\bar{x}, \bar{y})$ confined to some large compact set A, is given in Figure 15. The dotted line represents the "crossing" of ∂A. We also indicate the number of limit cycles in the different strata. The further analysis of the bifurcation diagram of X_λ in the focus case will be postponed to the next chapter, where we will have to introduce a new technique.

Before that we present, merely for the sake of completeness, some results in the elliptic case.

3.3 The elliptic case $(\varepsilon_1 = -1, b > 2\sqrt{2})$

Let us recall the (normal form) expression of a generic 3-parameter family unfolding a codimension 3-nilpotent singularity of elliptic type :

$$X_\lambda = y\frac{\partial}{\partial x} + (-x^3 + \mu_2 x + \mu_1 + y(\nu + b(\lambda)x + x^2 + x^3 h(x, \lambda) + y^2 Q(x, y, \lambda))\frac{\partial}{\partial y}$$

with $\lambda = (\nu, \mu_1, \mu_2)$.

One can show that the bifurcation diagram for $(\lambda, (x, y)) \in W \times V$, with W and V neighbourhoods of the origin (in λ-space and the (x, y)-plane, respectively), depends on the specific shape of V. Moreover, once V is chosen, the germ of the bifurcation diagram at 0 does depend on the family X_λ itself and not only on the germ of X_λ at 0 (see [DRS2] for more details). The simplest possible bifurcation diagram (see Figure 17) is obtained when taking V to be a genuine round disc in the normal coordinates (i.e. coordinates in which X_λ has the expression given above, see Figure 16). Figure 17 shows again the intersection of the cone-like bifurcation diagram with a sphere around the origin.

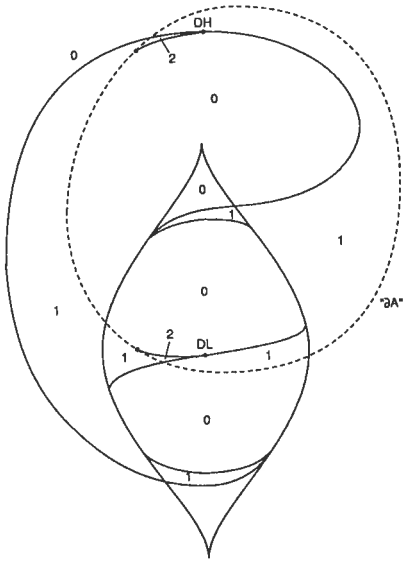

Figure 15 : Partial bifurcation diagram for the focus case

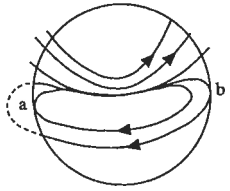

Figure 16 : A good choice of neighbourhood in normal coordinates

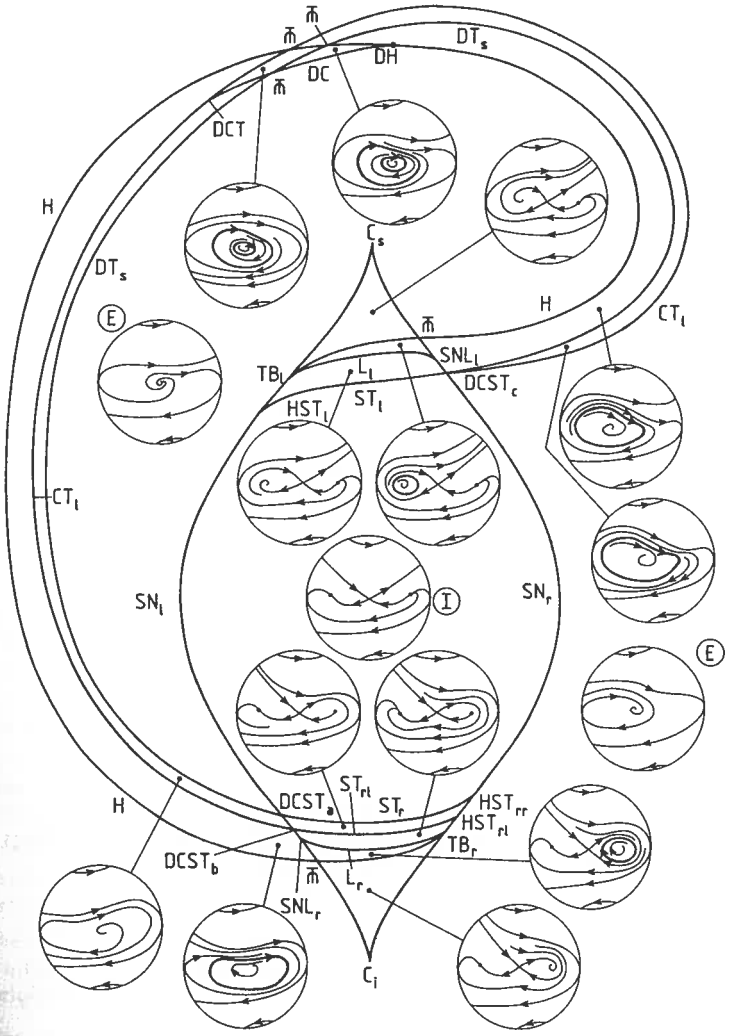

Figure 17 : Bifurcation diagram for the elliptic case

Some lines represent bifurcations that are linked to boundary behaviour like e.g. a (single or double) limit cycle touching the boundary ∂V, a (saddle or saddle-node) separatrix touching ∂V etc.

Everything has been proved, except for some bifurcations at the boundary, where it can be expected that a technique as presented in chapter 4 will finish the job. At least for the related Liénard equations the proof is complete. We show the result in Figure 18.

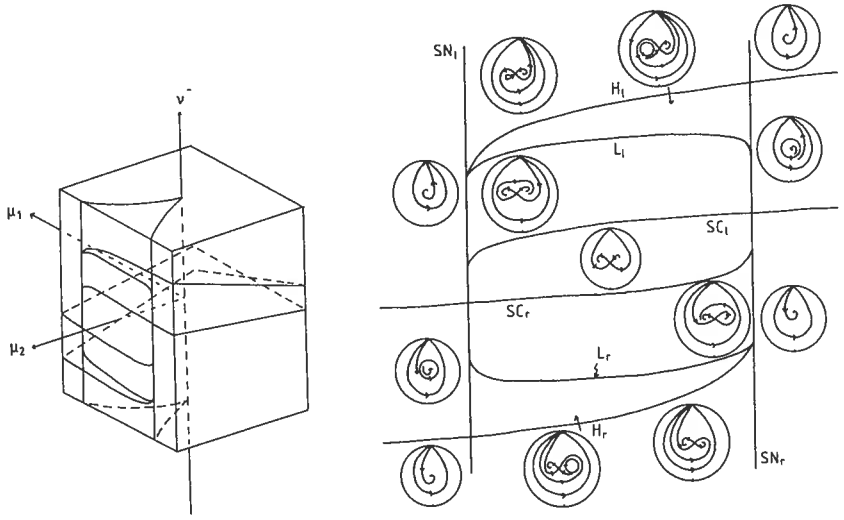

Figure 18 : Bifurcation diagram for the Liénard equations of elliptic type

4 Blow-up of families in the study of the nilpotent focus of codimension 3

Let us come back to the study of the nilpotent focus of codimension 3 :

$$X_\lambda = y\frac{\partial}{\partial x} + (-x^3 + \mu_2 x + \mu_1 + y(\nu + b(\lambda)x + x^2 + x^3 h(x,\lambda) + y^2 Q(x,y,\lambda))\frac{\partial}{\partial y}$$

with $\lambda = (\nu, \mu_1, \mu_2), b, h$ and Q are C^∞, $Q = O(||(x,y,\lambda)||^N)$ for some large N, and $0 < b(0) < 2\sqrt{2}$.

At the end of section 3.2 we obtained some "partial" bifurcation diagram, as shown in Figure 15, in which we have a dotted line representing the fact that a limit cycle can escape from a large compact region A in the $(\bar{x}, \bar{y})$-plane. We now wonder what this represents in the original coordinates (x, y). (Recall that $(x, y) = (r\bar{x}, r^2\bar{y})$.)

If we take $A = \{(\bar{x}, \bar{y}) | \bar{x}^4 + \bar{y}^2 \leq C\}$ for some $C > 0$, then $(\bar{x}, \bar{y}) \in A$ implies that

$$(x, y) \in A_r = \{(x, y) | x^4 + y^2 \leq Cr^4\}.$$

The smaller $r > 0$, the smaller is the domain A_r on which we know the phase portrait and on which we keep control of the limit cycles.

Let us keep in mind that we need to study the phase portraits of X_λ on some arbitrarily small fixed (with respect to $\lambda \in W$) neighbourhood V of the origin in the (x, y)-plane. Surely we can take V in such a way that X_0 is everywhere transverse to the boundary (see Figure 19).

Figure 19 : X_0 is transverse to ∂V

A limit cycle escaping from A_r is hence bound to stay in V. The study of these limit cycles has been done in [DR] and is based on the technique of blowing up families of vector fields (blowing up the unfoldings), a method introduced by R. Roussarie. It will be studied quite extensively in his notes ([R]) and then applied to a number of problems. As it seems to be a quite promising technique in local (and global) bifurcation theory we want to pay a lot of attention to it.

In appendix 2 we present the method — for didactical purposes — in a very simple situation where there is absolutely no need to use it, but where it is possible to see quite easily how it works.

In this section we use it to finish the study of the nilpotent focus of codimension 3, and in the next chapter we will use it to make a geometric description and analysis of a singular perturbation problem (relaxation equation).

The method consists in considering the family X_λ as a single vector field on $\mathbb{R}^5$ and to use a quasi-homogeneous blow-up at the origin. The most appropriate one for this case is (cf. principal rescaling) :

$$\begin{cases} x = r\bar{x} \\ y = r^2\bar{y} \end{cases} \qquad \begin{cases} \nu = r\bar{\nu} \\ \mu_1 = r^3\bar{\mu}_1 \\ \mu_2 = r^2\bar{\mu}_2 \end{cases} \qquad t = \bar{t}/r$$

with $\bar{x}^2 + \bar{y}^2 + \bar{\nu}^2 + \bar{\mu}_1^2 + \bar{\mu}_2^2 = 1$; it changes X into $\bar{X} = \frac{1}{r}\tilde{X}$.

The new vector field is no longer a family of planar vector fields, but outside the blown up $S^4 \times \{0\}$ we have an invariant 2-dimensional regular (analytic) foliation defined by the first integrals

$$\bar{\nu} r = \nu, \quad \bar{\mu}_1 r^3 = \mu_1, \quad \bar{\mu}_2 r^2 = \mu_2.$$

Later on it will become clear that this foliation extends to a regular analytic foliation everywhere outside $\{\bar{\nu} = \bar{\mu}_1 = \bar{\mu}_2 = 0, \bar{x}^2 + \bar{y}^2 = 1\}$. This fact will play a substantial role, but it is irrelevant for the moment.

As is often the case in working with blow-up we use "charts" in making specific calculations; the global view is only interesting for a complete and geometric presentation. The respective "charts" are given by :

(i) $\bar{\nu}^2 + \bar{\mu}_1^2 + \bar{\mu}_2^2 = 1$ and $(\bar{x}, \bar{y}) \in A$;

(ii) $\bar{x}^2 + \bar{y}^2 = 1$ and $\bar{\lambda} = (\bar{\nu}, \bar{\mu}_1, \bar{\mu}_2)$ in some open neighbourhood V of the origin.

In practice V is imposed — as we will see in this case too — by the calculations and will be rather small, while A will then be taken sufficiently large, in order to cover the rest.

The first chart gives exactly what we have called in chapter 3 the "(principal) rescaling of the family". A "blow-up of a family" gives an extension of the related rescaling. It is now clear that the limit cycles that escape from the domain A of the "rescaling chart" enter into the domain of the other chart. We will call this second chart "phase-directional rescaling" versus the usual "family rescaling" or "parameter-directional" rescaling.

As the domain of the first chart is diffeomorphic to $S^2 \times \mathbb{R}^2$ and the domain of the second to $S^1 \times \mathbb{R}^3$, it is also normal to use "subcharts" (generic charts this time) to make the calculation. In this process (cf. chapter 1) we sometimes have to divide by another positive function than r (e.g. $\bar{x}$ or $\bar{y}$). We now no longer represent $\bar{X}$ up to C^∞ conjugacy but up to C^∞ equivalence. This is no problem since we are only interested in phase portraits and not in precise time-estimation along the orbits (although by being more careful some results can be obtained). From this point of view it would be better to call $\bar{X}$ a "local vector field" (as R. Roussarie does) instead of a vector field but let us not be too formal in this example.

The calculations for (family) rescaling have been done in chapter 3, so let us turn to the "phase-directional rescaling". For simplicity we do not take $\bar{x}^2 + \bar{y}^2 = 1$ but $\bar{x}^4 + 2\bar{y}^2 = 1$, more precisely :

$$\bar{x} = Cs\theta, \quad \bar{y} = Sn\theta$$

where $Cs\theta$ and $Sn\theta$ are the solutions to the Cauchy problem :

$$\begin{cases} \dfrac{d}{d\theta} Cs\theta = -Sn\theta & Cs\theta = 1 \\ \dfrac{d}{d\theta} Sn\theta = Cs^3\theta & Sn\theta = 0 \end{cases}$$

Let us denote $Cs\theta = C$ and $Sn\theta = S$.

The operation leads to a vector field in $(\theta, r, \bar{\nu}, \bar{\mu}_1, \bar{\mu}_2)$-space, the θ-component of which is nowhere zero on $(r, \bar{\nu}, \bar{\mu}_1, \bar{\mu}_2) = (0, 0, 0, 0)$, thus representing a closed orbit. The Poincaré-map of the closed orbit with respect to the section $\{\theta = 0\}$ (whose fixed points will represent the different closed orbits) can be studied by means of the related θ-dependent vector field in $(r, \bar{\nu}, \bar{\mu}_1, \bar{\mu}_2)$; its expression is :

$$\begin{cases} r' = \dfrac{dr}{d\theta} = rV \\ \bar{\nu}' = \dfrac{d\bar{\nu}}{d\theta} = -\bar{\nu}V \\ \bar{\mu}_1' = \dfrac{d\bar{\mu}_1}{d\theta} = -3\bar{\mu}_1 V \\ \bar{\mu}_2' = \dfrac{d\bar{\mu}_2}{d\theta} = -2\bar{\mu}_2 V \end{cases}$$

with

$$V = \frac{bCS^2 + \bar{\mu}_2 SC + \bar{\mu}_1 S + \bar{\nu} S^2 + O(r)}{-1 + bC^2 S + \bar{\mu}_2 C^2 + \bar{\mu}_1 C + \bar{\nu} SC + O(r)} .$$

The special form of this vector field is imposed by the presence of the first integrals. Indeed :

$$\frac{\dot{\bar{\nu}}}{\bar{\nu}} = \frac{1}{2}\frac{\dot{\bar{\mu}}_2}{\bar{\mu}_2} = \frac{1}{3}\frac{\dot{\bar{\mu}}_1}{\bar{\mu}_1} = -\frac{\dot{r}}{r} .$$

These first integrals make it even possible to avoid the analysis of a 4-dimensional Poincaré-map and to study a 2-parameter family of 2-dimensional Poincaré-maps instead.

For this purpose we consider the following blowing up in parameter space :

$$\begin{cases} \bar{\nu} &= N\sigma \\ \bar{\mu}_1 &= M_1\sigma^3 \\ \bar{\mu}_2 &= M_2\sigma^2 \end{cases}$$

with $\sigma \geq 0$ and $(M_1, M_2, N) \in S^2$ or $\max(c_1|M_1|, c_2|M_2|, c_3|N|) = 1$ for some $c_1, c_2, c_3 > 0$. It is clear that the lines $\{(M_1\sigma^3, M_2\sigma^2, N\sigma) | \sigma > 0\}$ stay invariant when projecting the orbits of $\bar{X}$ on the parameter space. In other words, $\bar{X}$ respects the 3-dimensional spaces defined by $\{(\bar{x}, \bar{y}, M_1\sigma^3, M_2\sigma^2, N\sigma)\}$ for some fixed $(M_1, M_2, N) \in S^2$ and for $\sigma > 0$ (and even $\sigma \geq 0$). This remains true when we take $\sigma \geq 0$, and exactly the 2-spaces $\{(\bar{x}, \bar{y}, 0, 0, 0)\}$ obtained (in family rescaling) as limit of $\{(\bar{x}, \bar{y}, M_1 r^3, M_2 r^2, Nr)\}$ for $r \to 0$ together with $\{(x, y, 0, 0, 0) | (x, y) \neq (0, 0)\}$ provide the missing leaves of the extended regular foliation that we announced above (see the notes of R. Roussarie [R] for more details).

We have to study a family of Poincaré maps $(r, \sigma) \mapsto (R, \Sigma)$ described by θ-dependent (periodic) vector fields

$$\begin{cases} r' = Vr \\ \sigma' = -V\sigma \end{cases}$$

where $V = V(\theta, r, M_1\sigma^3, M_2\sigma^2, N\sigma)$ and (M_1, M_2, N) belongs to S^2 or ∂B for some cube B.

Again the Poincaré maps are quite special, since there is some invariant "foliation" defined by

$$R\Sigma = r\sigma.$$

This identity together with the symmetry due to the blow-up construction and given by

$$V(T/2 - \theta, -r, -\sigma) = -V(\theta, r, \sigma),$$

(where T is the period of S and C) make it easy to calculate — by integrating a system of non-homogeneous scalar linear differential equations — the asymptotic expansion of R :

$$R(r,\sigma) = r[1 + d_1 r + d_2 N\sigma + O(r^2) + O(r\sigma) + (d_3 M_1 + O(N, M_2)O(N))\sigma^3 + O(\sigma^4)]$$

with $d_1 < 0$, $d_2 < 0$ and $d_3 < 0$. The asymptotic expansion of Σ follows immediately from this, but is superfluous, because of the presence of the invariant foliation "$r\sigma = C$".

The asymptotic expression for R permits now quite easily to study the fixed points of the Poincaré map for $r > 0$. They are determined, within a certain leaf "$R\Sigma = r\sigma$", by the points r where the expression between brackets is equal to 1. In Figure 20 we represent the set of fixed points near $(r, \sigma) = (0, 0)$ of the Poincaré-map and this for varying (N, M_1), keeping $M_2 = 1$.

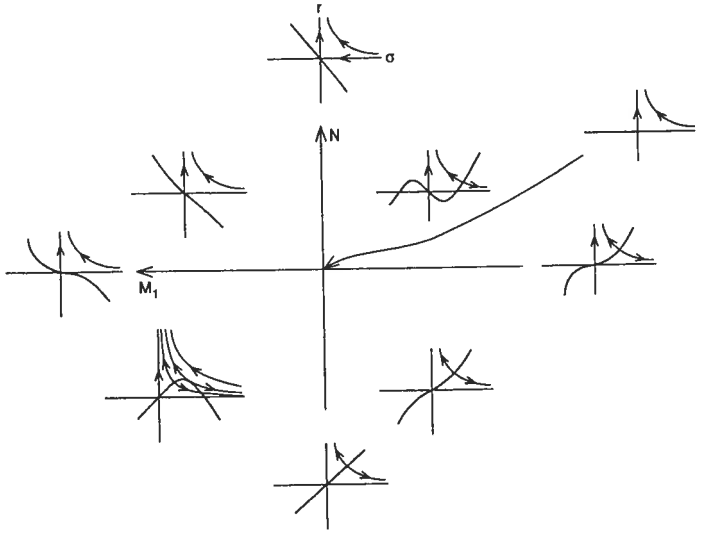

Figure 20 : Lines of fixed points in (r, σ)-plane

In Figure 21 we choose $r\sigma = C$ for $C > 0$ sufficiently small and show the bifurcation diagram of the fixed points (and hence related limit cycles) on $r\sigma = C$. All fixed points are hyperbolic or semi-hyperbolic of codimension 1, and all bifurcations are as generic as possible. These results are obtained by an asymptotic development, and are hence only valid for (r, σ) sufficiently small, let us say $0 < r \leq r_0$ and $a < \sigma < \sigma_0$. The dotted line in

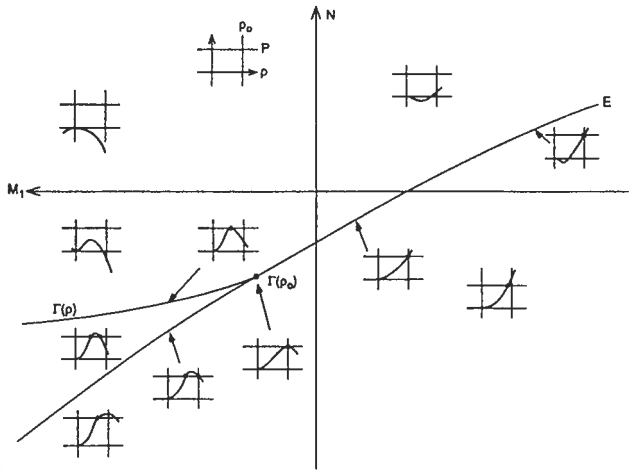

Figure 21 : Fixed points in $\{r\sigma = C\}$ and related bifurcation diagram

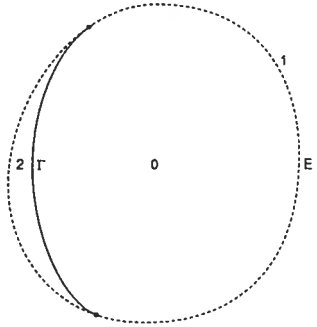

Figure 22 : Bifurcation diagram for the phase-directional chart

Figure 22 represents $\{r = r_0\}$ being crossed by a fixed point. The related limit cycle (for increasing r) leaves the domain where we can study it in the "phase-directional chart", but of course in the meantime is already in the domain of a "family rescaling chart" (since we choose A very large in this case).

Let us observe that in the different "phase-portraits" in Figure 20 the line $\{r = 0\}$ for $\sigma > 0$ represents a 1-dimensional section to the (Liénard type) vector field $\bar{X}^P_{\bar{\lambda}}$ near infinity in $(\bar{x}, \bar{y})$-plane, with $\bar{\lambda} = (N, M_1, M_2)$; the Poincaré-map restricted to $\{r = 0\}$ is indeed the Poincaré-map of $\bar{X}^P_{\bar{\lambda}}$ with respect to that section. The pictures clearly show how the Liénard vector fields can have at most one limit cycle (near infinity in $(\bar{x}, \bar{y})$-plane) while the vector fields X_λ can have two.

If we superpose Figure 15 and Figure 22, then the dotted line in both pictures (representing in fact the "passage" from one type of rescaling to the other) disappears and we get for X_λ (generic 3-parameter unfolding of a nilpotent focus of codimension 3) a bifurcation diagram as in Figure 23. Recall that everything is proved except for the remaining conjecture on the Liénard equation (see chapter 3 and [DRc]).

5 Singular perturbations and the "canard" phenomenon

In this last chapter we want to study the "canard (duck) phenomenon", occurring in Van der Pol's equation

$$\varepsilon\ddot{x} + (x^2 + x)\dot{x} + x - a = 0.$$

This phenomenon was first described and studied in [BCD] by means of non-standard analysis. Essentially it says that for sufficiently small $\varepsilon > 0$ and for decreasing a, the limit cycle created at $a = 0$ in a Hopf bifurcation stays for a while of "small size" (almost an equilibrium) before it very rapidly changes to a "big size" (near the relaxation oscillation shown in (5) of Figure 26). This change together with the occurrence of the intermediate shapes (called "canards" in [BCD], see also Figure 26) happens in a small interval $[a_1(\varepsilon), a_2(\varepsilon)]$ of which the length $|a_2(\varepsilon) - a_1(\varepsilon)| = O(e^{-k/\varepsilon})$ for some $k > 0$, when $\varepsilon \downarrow 0$.

In [DR] a geometric explanation and proof of this phenomenon in terms of standard analysis can be found. Essential ingredients of the method are foliations by center manifolds and blow-up of families. As the method is surely general enough to be used in other singular perturbation problems (relaxation equations), we will give a brief account of it in this chapter; we also give a precise (standard) description of the exact results in the Van der Pol case.

As usual we can reduce the second order scalar ODE to a first order system in the (x, Y)-plane, with $Y = \varepsilon\dot{x}$:

$$\begin{cases} \varepsilon\dot{x} &= Y \\ \dot{Y} &= a - x - \dfrac{Y}{\varepsilon}(x + x^2) \end{cases}.$$

Next, we use the Liénard transformation

$$y = Y + F(x) \text{ with } F(x) = \int_0^x (\xi + \xi^2)d\xi = \frac{x^2}{2} + \frac{x^3}{3}.$$

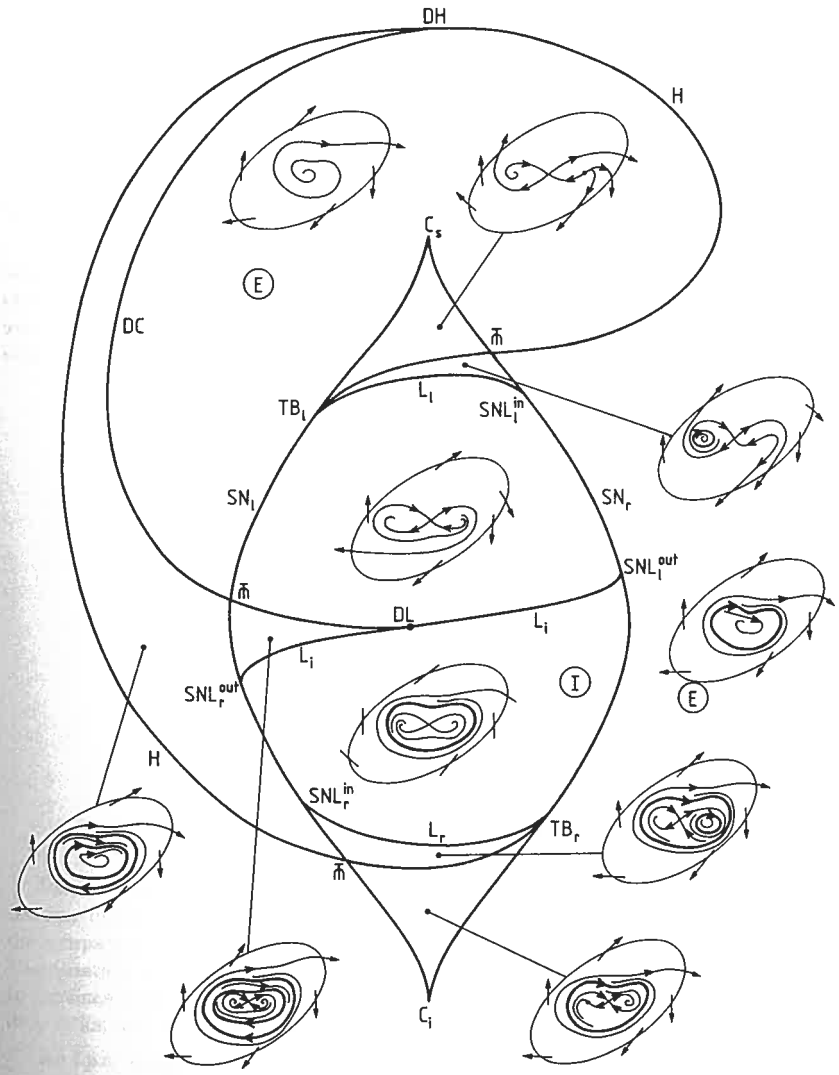

Figure 23 : Bifurcation diagram for the focus case

This transformation, together with the identity in the x-direction, gives a global diffeomorphism from the (x, Y)-plane to the (x, y)-plane, and changes the equation into :

$$\begin{cases} \dot{x} = \frac{1}{\varepsilon}(y - F(x)) \\ \dot{y} = a - x \ . \end{cases}$$

We finally rescale the time by a factor $1/\varepsilon$ and get :

$$X_{\varepsilon,a} = \begin{cases} \dot{x} = y - \frac{x^2}{2} - \frac{x^3}{3} \\ \dot{y} = \varepsilon(a - x) \ . \end{cases}$$

For $\varepsilon = 0$, the vector field $X_{0,a} = X_0 = (y - F(x))\partial/\partial x$ has the curve $L = \{y = F(x)\}$ as a curve of zeroes, and outside L, X_0 is horizontal (see Figure 23). Except for the points $n = (-1, 1/6)$ and $s = (0, 0)$ all the singularities on L are normally hyperbolic : they have an eigenvalue different from zero, attracting along L_1 and L_3, and repelling along L_2 (see Figure 24).

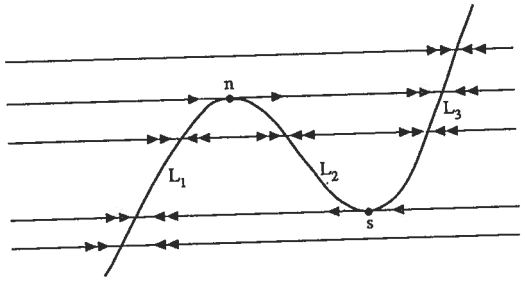

Figure 24 : Curve of zeroes of the vector field X_0

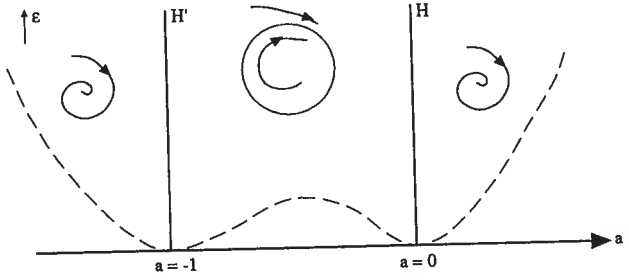

Figure 25 : Bifurcation diagram and phase portraits for $X_{\varepsilon,a}$ with $\varepsilon > 0$

From now on we will take $\varepsilon \geq 0$ and also $a \geq -1/2$, because of the symmetry given by $(x, y, a) \mapsto (-x - 1, -y + 1/6, -a - 1)$, which interchanges the role of the points s and n.

The bifurcation diagram for $X_{\varepsilon,a}$, with $\varepsilon > 0$, is quite simple and is given in Figure 25 together with the stable phase portraits as they appear in the complete (x, y)-plane. The lines H and H' represent generic supercritical Andronov-Hopf bifurcations. In between H and H' the vector field $X_{\varepsilon,a}$ has exactly one repelling hyperbolic singularity at $p_a = (a, F(a))$ and one attracting hyperbolic limit cycle $\Gamma_{\varepsilon,a}$ surrounding it, while outside this region the system only has an attracting hyperbolic singularity at $(a, F(a)) = p_a$. Above the dotted line (see Figure 25) the singularity is a focus, and beneath the dotted line it is a node. All these facts are easy to prove, using for instance the theorem of Coppel, as in chapter 3.

The kind of mathematical question that one can ask in view of the observations that we referred to in the beginning of this chapter is : *what happens to the limit cycle $\Gamma_{\varepsilon,a}$ when $\varepsilon \to 0$?*

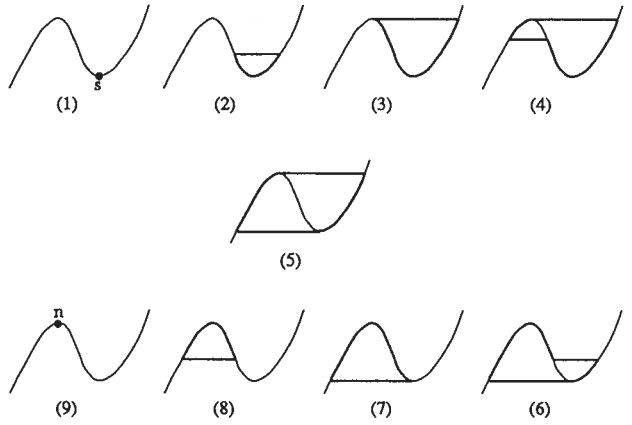

Figure 26 : List of limit periodic sets of X_0

We are especially interested in the limiting position of $\Gamma_{\varepsilon,a}$ when $\varepsilon \to 0$, depending on the way in which $(\varepsilon, a) \to (0, a_0)$. Such a limiting set for the Hausdorff distance between the compact sets in $\mathbb{R}^2$ (see [R] for more information) is called a *limit periodic set (l.p.s.)*. The question involves describing the possible limit periodic sets of X_0, and it is not hard to convince oneself that they are all shown in Figure 26. Let us stick to $a \geq -1/2$ in their description and further treatment, since the other cases are the "symmetric" counterparts.

An l.p.s. as in (1) is called "small" and is denoted by Γ_0, and one as in (2) is called "big" and denoted by Γ_B. The cases (2)-(4) are commonly called "canards" (ducks) because of the shape of the 4th case. Let us call them respectively l.p.s. of type I (canard sans tête (without a head)), l.p.s. of type II (canard à petite tête (with a small head)) and l.p.s. of type III (canard avec tête (with a head)).

For the cases of type I and III we make a distinction as in Figure 27, denoting them by Γ_y^I and Γ_y^{III}.

Let us remark that $\Gamma_0^I = \Gamma_0$, $\Gamma_0^{III} = \Gamma_B$ and $\Gamma_{1/6}^I = \Gamma_{1/6}^{III} = \Gamma^{II}$. We are now ready to make a precise statement of the so-called "canard phenomenon".

We define $k(y) = \int_0^{x(y)} x(1+x)^2 dx$, where $x(y)$ is the largest negative solution of $\{\frac{x^2}{2} + \frac{x^3}{3} = y\}$ and $y \in [0, 1/6]$. The function k is C^1, $k'(y) = 1 + x(y)$, k is analytic on $]0, 1/6[$, $k(0) = 0$ and $k(1/6) = 1/12$.

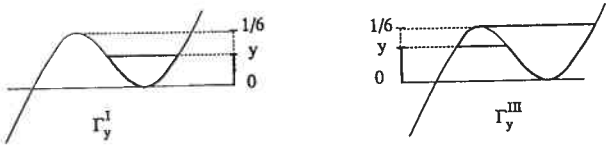

Figure 27 : Different "canards"

Theorem 1 (see [DR3]) *There exists a curve $C_0 = \{a = c_0(\varepsilon)\}$ with $c_0(\varepsilon) = \sqrt{\varepsilon}\ \bar{a}(\sqrt{\varepsilon})$ and $\bar{a}$ a C^∞-function with $\bar{a}'(0) = -1$ such that for any continuous curve $C = \{a = c(\varepsilon)\}$ with $c(\varepsilon) \leq 0$ and $c(0) \in [-1/2, 0]$ we have :*

(1) $\lim_{\varepsilon\to 0} \Gamma_{\varepsilon,c(\varepsilon)} = \Gamma_0 \iff$ *for small $\varepsilon > 0$: $c(\varepsilon) > c_0(\varepsilon)$ and* $\overline{\lim}(-\varepsilon \log(c(\varepsilon) - c_0(\varepsilon))) \leq 0$;

(2) $\lim_{\varepsilon\to 0} \Gamma_{\varepsilon,c(\varepsilon)} = \Gamma_y^I \iff$ *for small $\varepsilon > 0$: $c(\varepsilon) \geq c_0(\varepsilon)$ and* $\lim(-\varepsilon \log(c(\varepsilon) - c_0(\varepsilon))) = k(y)$;

(3) $\lim_{\varepsilon\to 0} \Gamma_{\varepsilon,c(\varepsilon)} = \Gamma^{II} \iff \underline{\lim}(-\varepsilon \log|c(\varepsilon) - c_0(\varepsilon)|) \geq k(1/6)$;

(4) $\lim_{\varepsilon\to 0} \Gamma_{\varepsilon,c(\varepsilon)} = \Gamma_y^{III} \iff$ *for small $\varepsilon > 0$: $c(\varepsilon) \leq c_0(\varepsilon)$ and* $\lim(-\varepsilon \log(c_0(\varepsilon) - c(\varepsilon))) = k(y)$;

(5) $\lim_{\varepsilon\to 0} \Gamma_{\varepsilon,c(\varepsilon)} = \Gamma_B \iff$ *for small $\varepsilon > 0$: $c(\varepsilon) < c_0(\varepsilon)$ and* $\overline{\lim}(-\varepsilon \log(c_0(\varepsilon) - c(\varepsilon))) \leq 0$.

It is hence clear that in order to obtain a l.p.s. of canard type as limit of a 1-parameter family of limit cycles $\Gamma_{\varepsilon,\gamma(\varepsilon)}$ we have to choose a $\gamma(\varepsilon)$ having a flat contact with $c_0(\varepsilon)$. The precise asymptotics are also described.

Another way to present the "canard phenomenon", more emphasizing the visual observation, consists of the following :

Theorem 2 (see [DR3]) *For each $\delta > 0$, there exists $\varepsilon_0(\delta) > 0$ and $K(\delta) > 0$ such that for $0 < \varepsilon < \varepsilon_0(\delta)$, one necessarily has $a \in [c_0(\varepsilon) - e^{-K(\delta)/\varepsilon},\ c_0(\varepsilon) + e^{-K(\delta)/\varepsilon}]$ when one of the following conditions holds :*

$$d(\Gamma_{\varepsilon,a}, \Gamma_y^I) < \delta/2 \quad \textit{with} \quad y \in [\delta, 1/6]$$

or

$$d(\Gamma_{\varepsilon,a}, \Gamma_y^{III}) < \delta/2 \quad \textit{with} \quad y \in [\delta, 1/6].$$

In the rest of this chapter we will now try to give a short survey of the proof of both theorems, indicating the main ideas, such as the use of (foliations by) center manifolds and desingularization (blow-up) of a family.

Let us first have a closer look at the normally hyperbolic points on $L_1 \cup L_2 \cup L_3$ (see Figure 24).

At each such point p we know by a theorem of Takens (see [T2], or [B] for an extension to families) that for all $k \in \mathbf{N}_1$ the 3-dimensional vector field (or 1-parameter family of 2-dimensional vector fields) is locally C^k-equivalent to the following normal form :

$$\pm\bar{y}\frac{\partial}{\partial\bar{y}} + \varepsilon\frac{\partial}{\partial\bar{x}} .$$

Along L_2 there is a $(-)$-sign, and along $L_1 \cup L_3$ a $(+)$-sign. Let us go on along L_2 (the other case being similar). In fact, the theorem of Takens (or its extension) only provides a C^k "normal-linearization" but the fact that $\frac{\partial X_{0,\varepsilon}}{\partial\varepsilon}(p) \neq 0$ permits very easily to produce the simple expression.

If in these coordinates we consider any line segment

$$C = (\bar{x}_0(\varepsilon), \bar{y}_0(\varepsilon))$$

with $\bar{y}_0(0) > 0$ and we take the saturation by means of the flow, then its closure defines a C^k center manifold at each point $(\bar{x}, 0)$ with $\bar{x} > \bar{x}_0(0)$. The center manifold is explicitly defined by

$$\bar{y}(\varepsilon, \bar{x}) = \bar{y}_0(\varepsilon) \exp\left(\frac{\bar{x}_0(\varepsilon) - \bar{x}}{\varepsilon}\right).$$

It is the graph of a C^k function $\bar{y}$ which is k-flat along $\{\varepsilon = 0\}$.

Let us now look at the l.p.s. of type I, together with the related "canard" limit cycles. For this we will construct "center manifolds".

In order to get some feeling of the construction we suppose that the parameter a stays zero ($a = 0$), so that we are left with a unique parameter ε.

At "height" $0 < y_0 < 1/6$ (see Figure 27) we consider a straight line segment $\{y = y_0, x = 0\}$ in (x, y, ε)-space, and we saturate it in forward and backward time with the flow of $(X_{0,\varepsilon}, \dot{\varepsilon} = 0)$; let W_{y_0} be the closure of this saturation.

The interesting fact to observe is that (as long as we stay in $\{y > 0\}$) W_{y_0} is a C^∞ manifold except at the points $(x_0^\pm, F(x_0^\pm) = y_0)$. At all points $(x, F(x))$, with $x > -1$ and

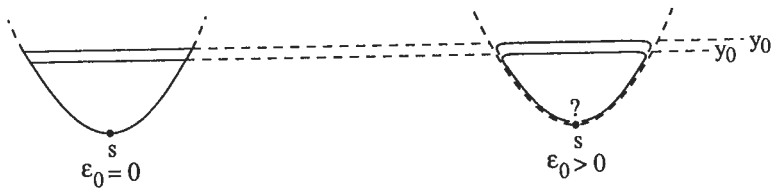

Figure 28 : Intersection of W_{y_0} with $\{\varepsilon = \varepsilon_0\}$

$0 < y = F(x) < 1/6$, W_{y_0} is a C^∞ center-manifold for $(X_{0,\varepsilon}, 0)$. The intersection of W_{y_0} with $\{\varepsilon = 0\}$, and with $\{\varepsilon = \varepsilon_0\}$ for small $\varepsilon_0 > 0$, are represented in Figure 28, respectively in the left and in the right picture. As we can do this for all $0 < y_0 < 1/6$, we obtain a foliation by center manifolds, namely $\{W_{y_0}\}$. This foliation is "singular" on $\{\varepsilon = 0\}$ but its intersection $\{W_{y_0}^{\varepsilon_0}\}$ with each plane $\{\varepsilon = \varepsilon_0\}$; for $\varepsilon_0 > 0$, it defines a genuine regular C^∞ foliation in some open domain. The different $\{W_{y_0}\}_{0<y_0<1/6}$ mutually have a flat contact along $\{(x, F(x)), \varepsilon = 0\}$ whenever they are defined.

In reality we must not forget the parameter a, implying that we will have a similar foliation for each a separately, everything depending smoothly on a.

The hard part of the analysis starts when we want to see what happens to W_{y_0} when it arrives at s (see Figure 28), in forward as well as in backward time. To that end we will use — as in chapter 5 — a blow-up of the family $X_{\varepsilon,a}$ at the point $s_0 = (0,0,0,0)$; we call it Φ and it is given by :

$$x = u\bar{x}, \quad y = u^2\bar{y}, \quad \varepsilon = u^2\bar{\varepsilon}, \quad a = u\bar{a},$$

with $\bar{x}^2 + \bar{y}^2 + \bar{\varepsilon}^2 + \bar{a}^2 = 1$, $\varepsilon \geq 0$.

We write $\bar{X} = \frac{1}{u}(\Phi_*^{-1}(X))$, for $X = X_{\varepsilon,a}$.

Again for the calculation, we use different charts (see chapter 5 and appendix 3)

(i) Family rescaling :
$(\bar{x}, \bar{y}) \in D$, some large compact set, and respectively :

$$\begin{cases} \text{(a)} & \bar{\varepsilon} = 1, \quad \bar{a} \in [-A_0, A_0] \\ \text{(b)} & \bar{\varepsilon} \sim 0, \quad \bar{a} = \pm 1 \end{cases}$$

with $A_0 > 0$ large.

(ii) Phase-directional rescaling
$\bar{x} = Cs\theta, \bar{y} = Sn\theta$ (hence $\bar{x}^4 + 2\bar{y}^2 = 1$)
$(\bar{a}, \bar{\varepsilon}) \sim (0,0)$.
(see chapter 4 for the definition of $Cs\theta$ and $Sn\theta$; as in chapter 4 we will use "subcharts" in this case).

In Figure 29 we show the desingularization of the singularity in $(\bar{x}, \bar{y})$-plane (phase-directional rescaling for $(\bar{a}, \bar{\varepsilon}) = (0,0)$). As we already observed in chapter 5, the phase-

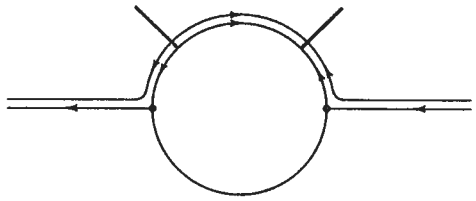

Figure 29 : Blow-up of X_0 at $(0,0)$

directional rescaling gives the phase-portrait "at infinity" for the "compactification" of the family rescaling. With respect to that family rescaling we will obtain different limiting phase portraits (for $u \downarrow 0$) in the $(\bar{x}, \bar{y})$-plane, depending on the different values $(\bar{\varepsilon}, \bar{a})$ with $\bar{\varepsilon}^2 + \bar{a}^2 = 1$. In Figure 30 we draw the "compactification" of these phase portraits (on a Poincaré hemisphere). All pictures are desingularized except when $\bar{\varepsilon} = 0$; in that case we need to perform an extra blow up, along the line $(\bar{\varepsilon}, \bar{x}, \bar{y}) = (0,0,0)$. In Figure 31 we depict again the $(\bar{\varepsilon} = 0)$-case, this time with the origin blown up. The pictures in Figure 30 show

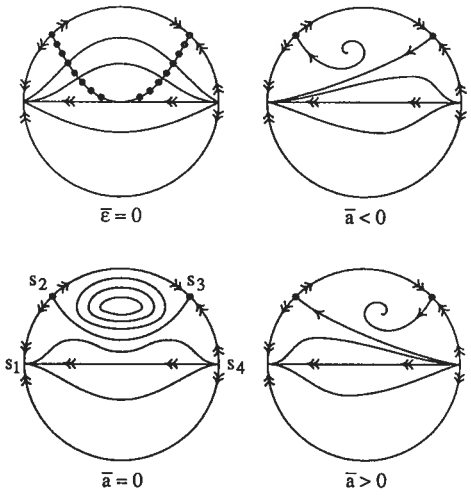

Figure 30 : Compactified phase portraits of $\bar{X}_{\bar{\varepsilon},\bar{a}}$ in the family rescaling

$\bar{X}$ on well-chosen 2-manifolds (with boundary) within $\{u = 0\}$. The question remains on how they are connected to the blow-up of the singularity as represented in Figure 29. All this happens in a 4-dimensional space, but as we already observed in chapter 4, the total space can be decomposed as a 1-parameter family of 3-dimensional invariant spaces $P_{(E,A)}$ with $(E, A) \in S^1$ (or (E, A) belonging to the boundary of a rectangle), and $P_{(E,A)}$ representing the part of the total space that projects onto the line

$$\{(\bar{\varepsilon}, \bar{a}) = (v^2 E, vA) | v \geq 0\}.$$

In Figure 32 we represent such an invariant $P_{(E,A)}$ near the circle segment (on $(\bar{\varepsilon}, \bar{a}) = (0, 0)$, $\bar{x}^2 + \bar{y}^2 = 1$) connecting s_2 and s_3. From now on we will make the calculations in each $P_{(E,A)}$ separately (keeping in mind the dependence on (E, A)) using the coordinates (θ, u, v)

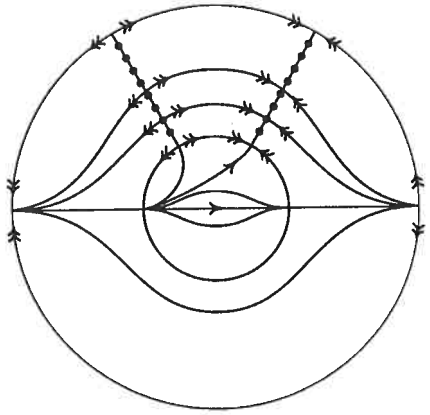

Figure 31 : Desingularized phase portraits of $\bar{X}_{0,\pm 1}$

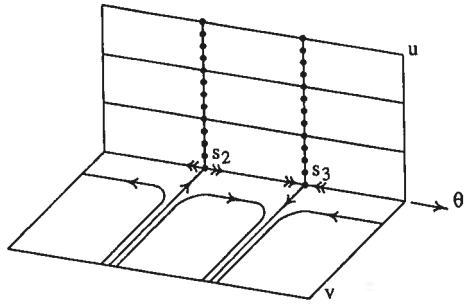

Figure 32 : A 3-dimensional subspace in the phase-directional rescaling

as introduced above. In a "chart" with $E = 1$ (side of a rectangle) we find :

$$\begin{cases} \dot{u} = v^2 v_1(\theta, v, u, A)u \\ \dot{v} = -v^2 v_1(\theta, v, u, A)v \\ \dot{\theta} = v_1(\theta, v, u, A), \end{cases}$$

respecting the foliation defined by $\{uv = C\}$.

To follow now the center manifolds W_{y_0}, as they pass through s_2 and s_3, we can use the "normal form" :

$$-z\frac{\partial}{\partial z} + v^2 f(u, v, A)(-u\frac{\partial}{\partial u} + v\frac{\partial}{\partial v}),$$

or equivalently (for C^k-equivalence) :

$$-u\frac{\partial}{\partial u} + v\frac{\partial}{\partial v} - \frac{z}{v^2 f}\frac{\partial}{\partial z}$$

with $f(u, v, A) > 0$. We easily see that the W_{y_0} stay C^∞ at s_2 and s_3, and even beyond s_2 and s_3 (near $(z, u) = (0, 0)$) in forward and backward time, respectively. To see how they further evolve for increasing and decreasing t, we can use the family rescaling (see the pictures in Figure 30). In Figure 33 we show a global 3-dimensional view of a W_{y_0} for $(\bar{\varepsilon}, \bar{a})$

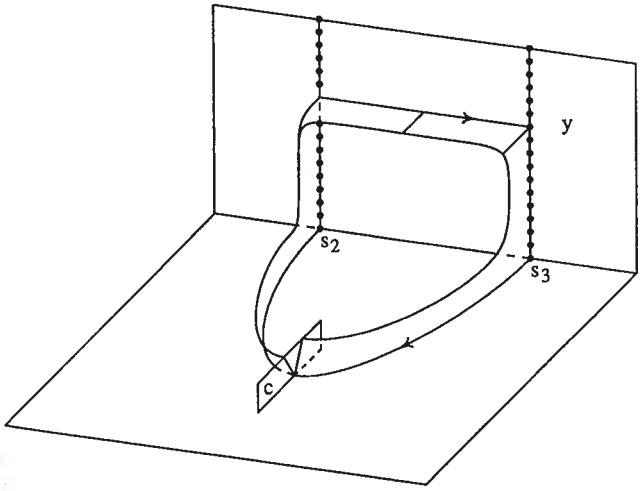

Figure 33 : Global 3-dimensional view of some W_{y_0}

$= (1,0)$. We also represent the intersection in forward — and backward — time with some transverse section C. As coordinates on this section C we use (u,h) with u the "distance parameter" in the rescaling (blow-up) and h the value of the Hamiltonian related to the vector field at $(\bar{\varepsilon},\bar{a}) = (1,0)$. This vector field is the time reversible

$$X_S = (\bar{y} - \frac{\bar{x}^2}{2})\frac{\partial}{\partial \bar{x}} - \bar{x}\frac{\partial}{\partial \bar{y}},$$

having $e^{-\bar{y}}$ as integrating factor and

$$H(\bar{x},\bar{y}) = -e^{-\bar{y}}(\bar{y} - \frac{\bar{x}^2}{2} + 1)$$

as related Hamiltonian. At the center $H(0,0) = -1$, and along the saddle-connection $\Gamma = \{\bar{y} = \frac{1}{2}\bar{x}^2 - 1\}$ we have $H(\Gamma) = 0$. If we look at the related dual 1-form $\omega_{u,\bar{a}}$, we get :

$$e^{-\bar{y}}\omega_{u,\bar{a}} = dH - e^{-\bar{y}}(\bar{a}d\bar{x} + \frac{u}{3}\bar{x}^3 d\bar{y})$$

The Poincaré mapping with respect to $\{\bar{x} = 0\}$, and for $-1 < h < 0$, is given by (compare with appendix 2) :

$$P_{u,\bar{a}}(h) = h + \bar{a}I_1(h) + uI_2(h) + o(|\bar{a},u|)$$

with

$$I_1(h) = \int_{\Gamma_h} e^{-\bar{y}}d\bar{x}, \quad I_2(h) = \frac{1}{3}\int_{\Gamma_h} e^{-\bar{y}}\bar{x}^3 d\bar{y}$$

and $\Gamma_h = H^{-1}(h)$ (e.g. $\Gamma_0 = \Gamma$ and $\Gamma_{-1} = (0,0)$); moreover,

$$\frac{I_2(0)}{I_1(0)} = 1, \quad I_1(0) < 0 \quad \text{and} \quad \lim_{h\to -1}\frac{I_2(h)}{I_1(h)} = 0.$$

The "small" limit cycles will have as "limiting set" a periodic orbit of X_S, and they occur along curves with slope

$$\bar{a}I_1(h) + uI_2(h) = 0\ ,$$

e.g. for the Hopf bifurcation the slope is $\bar{a} = 0$.

The "canard" limit cycles will all occur along lines with slope

$$\bar{a}/u = -I_2(0)/I_1(0) = -1\ .$$

Of course this last statement needs a proof, and it is technical and quite long (see [DR3]). In Figure 34 we draw the forward and backward intersection of W_{y_0} with C (which we represent by $h = F(u,A,y_0)$ and $h = B(u,A,y_0)$, respectively), and show how they evolve with respect to A. One can show :

$$F(u,A,y_0) - B(u,A,y_0) = I_1(0)[A + u + o(|A,u|)]\ .$$

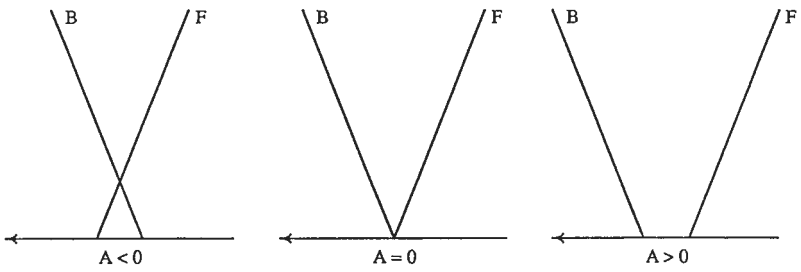

Figure 34 : Forward and backward intersection of W_{y_0} with C

The intersection of B and F for $A < 0$ gives a "canard" limit cycle (of type I) close to the limit periodic set $\Gamma^I_{y_0}$.

The fact that all "canard" limit cycles are very close to each other is a consequence of the mutual flat contact between the center manifolds W_{y_0}. This flat contact can be described in a rather precise way after choosing a single center manifold as a reference. At this stage and in order to include also the study of l.p.s. of type II and III we prefer to take one of type II as reference (only such a choice agrees with the statement of Theorem 1).

However, an l.p.s. of type II contains also the point n and in order to construct the necessary center manifolds and to follow them, where needed, we will have to blow up at the point $n_0 = (-1,1/6,0,0)$ too. To fit with the blow-up at s_0 we use

$$(x,y,\varepsilon,a) = (u'^2x', u'^4y', u'^6\varepsilon', u'^3a').$$

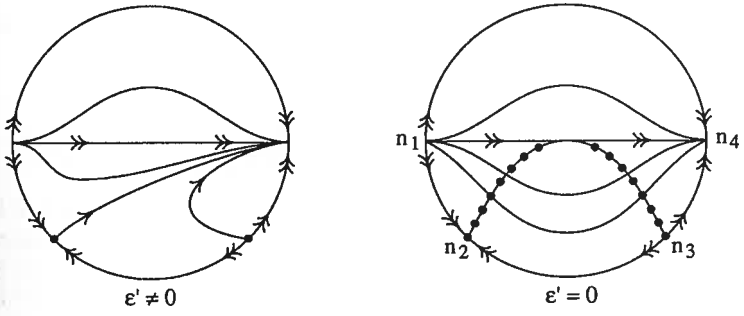

Figure 35 : Compactified phase portraits in the family rescaling at n_0

In the interesting directions (ε', a') with $\varepsilon' \neq 0$, e.g. $\varepsilon' = 1$, this leads to a desingularization. In Figure 35 we show the compactification of the resulting phase portraits for the family rescaling. In Figure 36 we sketch a "center manifold" W obtained by choosing a line segment transverse to the picture in Figure 35, saturating it in forward and backward time, and taking the closure. Such a center manifold will be everywhere C^∞ except possibly along the X_0-orbit connecting n_4 and n'_4.

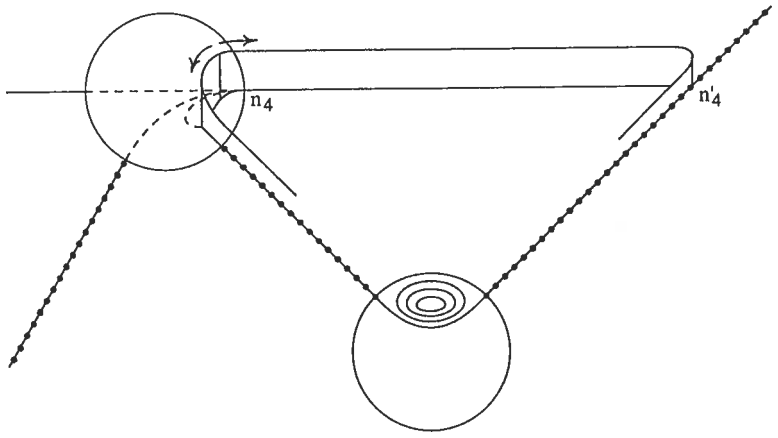

Figure 36 : Global 3-dimensional view of some center manifolds through n

Let us represent the intersection of W with C by $\{h = F_{II}(u, A)\}$ and $\{h = B_{II}(u, A)\}$. It can now be proved that

$$B_{II}(u, A) - B(u, A, y_0) = \exp(-\frac{k_B(y_0, A)}{u^2}(1 + O(u))),$$

$$F_{II}(u, A) - F(u, A, y_0) = \exp(-\frac{k_F(y_0, A)}{u^2}(1 + O(u)))$$

with k_B and k_F both positive C^∞ functions, and $k_F(y_0, 0) > k_B(y_0, 0)$ for $y_0 \in]0, 1/6[$.

If we denote

$$\Delta_0(u, A) = F_{II}(u, A) - B_{II}(u, A)$$

and

$$\Delta(u, A, y_0) = F(u, A, y_0) - B(u, A, y_0) = \Delta_0(u, A) + \Phi(u, A, y_0),$$

then it follows by the implicit function theorem that

$$\Delta = 0 \iff A = A(u, y_0)$$
$$\Delta_0 = 0 \iff A = A_0(u)$$

One can now prove that

$$A(u, y_0) = A_0(u) + \exp\left(-\frac{k_B(y_0, 0)}{u^2}(1 + O(u))\right)$$

and $k_B(y, 0) = k(y)$ in the statement of Theorem 1.

Let us remark that this survey of the proof was rather quick (especially in the last steps) and quite incomplete concerning the technical elaboration. We must also not forget to do something similar for the limit periodic sets of type III but here the techniques are the same as in the previous study.

Appendix 1 Perturbation from a Hamiltonian and the nilpotent saddle of codimension 3

As announced in chapter 3, we present this general principle in the specific situation occurring for the nilpotent saddle of codimension 3. We leave out technical details, however. Recall that (omitting primes and taking $v = 1$) the 1-form $(K\omega)_{(\mu_1,\nu,\tau)}$ was given by

$$K\omega = dH - \tau K(\mu_1 + \nu y + x^2 y)dx + o(\tau) .$$

We want to study $K\omega$ (or the related family of vector fields) on a domain N in (x, y)-plane as depicted in Figure 37.

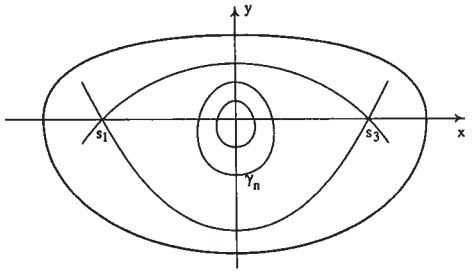

Figure 37 : Domain in the (x, y)-plane to study ω

Perturbation Lemma *Let $(K\omega)_{(\mu_1,\nu,\tau)}$ be the 1-form given above and let L be a compact subset of the (μ_1, ν)-plane. Then there exists a value $T(L) > 0$ such that for all $(\tau, \mu_1, \nu) \in [0, T(L)] \times L$ we have the following properties :*

(i) *$(K\omega)_{(\mu_1,\nu,\tau)}$ admits only three singularities in N of which two (s_1 and s_3) are saddles, while the third one s_2 is an anti saddle (center or focus).*
The first return map $P_{(\mu_1,\nu,\tau)}$ (or its inverse) is defined on the entire segment $]s_2, s_3[$.

(ii) *If we parametrize* $[s_2, s_3]$ *using the value of the function* H *we obtain a parametrization (in a variable* h*) which is regular on* $]H(s_2), H(s_3)[$*. For this parametrization, the mapping* $P_{(\mu_1,\nu,\tau)}$ *has the following development on its domain of definition :*

$$P_{(\mu_1,\nu,\tau)}(h) = h + \tau \int_{\gamma_h} K(\mu_1 + \nu y + x^2 y)dx + o(\tau) \ ,$$

where γ_h *is the compact component of* $\{H = h\}$ *clockwise oriented for the integration (and something similar for* $P^{-1}_{(\mu_1,\nu,\tau)}$*).*

Hence up to first order, the study of the limit cycles corresponds to the study of solutions of the integral equation

$$\mu_1 \int_{\gamma_h} K dx + \nu \int_{\gamma_h} K y dy + \int_{\gamma_h} K x^2 y dy = 0 \ .$$

The study of these "Abelian integrals" has been done in [Z] and is highly nontrivial. On the regular parts of H (given by some compactum in $]s_2, s_3[$), the implicit function theorem allows us to show that the picture for $\tau = 0$ persists as $\tau > 0$. A somewhat more involved argument — not included herein — derives the same conclusion at the point s_2. At the value $H(s_3)$, the limit situation described by the integral equation does not persist. Nevertheless it is possible to make the study over there as well, though the price is another lengthy calculation (see [DRS2]).

The bifurcation diagram (of the limit cycles) of $K\omega$ for $\tau > 0$ is shown in Figure 38 to the left, while the limiting position for $\tau = 0$ (describing the bifurcation diagram of the zeroes of the integral equation) is shown in Figure 38 to the right.

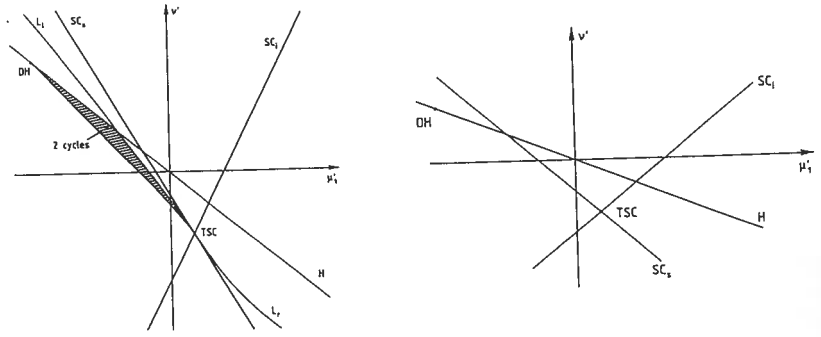

Figure 38 : Bifurcation diagram for limit cycles ($\tau > 0$) and for zeroes of the integral expression ($\tau = 0$)

Appendix 2 Blow up of families and the Andronov-Hopf bifurcation

As announced in chapter 4 we present here the method of "blowing up a family" — for didactical purposes — in the study of the well known Andronov-Hopf bifurcation. Let us take it for granted that the study of this phenomenon can be reduced — by normal form theory and for the notion of C^∞-equivalence — to the family

$$(x\frac{\partial}{\partial y} - y\frac{\partial}{\partial x}) + (\lambda + (x^2+y^2) + (x^2+y^2)^2 g((x^2+y^2),\lambda) + h(x,y,\lambda))(x\frac{\partial}{\partial x} + y\frac{\partial}{\partial y}) \ ,$$

where $\lambda \in \mathbb{R}$, h and g C^∞ and $j_\infty h(0,0,\lambda) = 0$.

We "blow up the unfolding" $X = X_\lambda$, using the homogeneous transformation ϕ, given by

$$(x, y, \lambda) = (r\bar{x}, r\bar{y}, r\bar{\lambda})$$

with $\bar{x}^2 + \bar{y}^2 + \bar{\lambda}^2 = 1$.

In this way, the three-dimensional vector field $X(x,y,\lambda) = X_\lambda(x,y)$ is changed into $\tilde{X}$ with $\phi_*(\tilde{X}) = X$ and the origin is substituted by the 2-sphere $S^2 = \{r = 0\}$. Just as in the blow-up method for singularities, we would change $\tilde{X}$ into $\bar{X} = \frac{1}{r^k}\tilde{X}$ (for $j_k X(0) = 0$ and $j_{k+1}X(0) \neq 0$), but this is not needed here.

An apparent disadvantage of the method is that, by treating parameters as variables, we loose the "family character" of X. Indeed, the invariant 2-planes $\{\lambda = \lambda_0\}$ for $\lambda_0 \neq 0$, are not changed into invariant 2-planes, but into leaves of an invariant 2-dimensional (curved) foliation, namely $E_{\lambda_0} = \{r\bar{\lambda} = \lambda_0\}$. The plane $\{\lambda = 0\}$ is changed into $E_0 = S^2 \cup (S^1 \times \mathbb{R}^+_0)$ and $\tilde{X}|S^1 \times \mathbb{R}^+_0$ is merely the usual polar blow-up of the vector field X_0.

The study can now be split into two parts by using "charts" :

A.2.1 Rescaling of the family

This is the traditional part of the blow-up method : we choose $\bar{\lambda} = \pm 1$ (or $\bar{\lambda} = \pm A$ if necessary) and confine $(\bar{x}, \bar{y})$ to a large compactum in the $(\bar{x}, \bar{y})$-plane :

$$(x, y, \lambda) = (r\bar{x}, r\bar{y}, \pm r) \ .$$

Moreover, because of the rotational symmetry in the problem, we can introduce polar coordinates :

$$\begin{cases} \bar{x} = s\cos 2\pi\eta \\ \bar{y} = s\sin 2\pi\eta \ . \end{cases}$$

This gives us the following expression for $\tilde{X}$ (in some C^∞-coordinates) :

$$\begin{cases} \dot{\eta} = 1 \\ \dot{s} = rs(\pm 1 + O(r)) \ . \end{cases}$$

Hence we obtain a global spiral sink (or source) in the phase plane $(\bar{x}, \bar{y})$ for $r > 0$, see Figure 39.

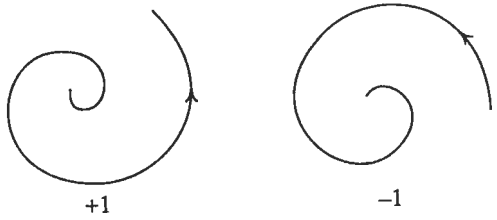

Figure 39 : Phase portraits after family rescaling

A.2.2 Phase directional rescaling

This is the new part of the blow-up method. We choose $\bar{x}^2 + \bar{y}^2 = 1$ and $\bar{\lambda} \sim 0$, and take

$$(x, y, \lambda) = (r\cos 2\pi\theta, r\sin 2\pi\theta, r\bar{\lambda}).$$

We find

$$\begin{cases} \dot{\theta} = 1 \\ \dot{r} = r^2 B(r, \theta, \bar{\lambda}) \\ \dot{\bar{\lambda}} = -\bar{\lambda} r B(r, \theta, \bar{\lambda}) \end{cases}$$

with

$$B(r, \theta, \bar{\lambda}) = \bar{\lambda} + r + r^3 g(r^2, r\bar{\lambda}) + \frac{1}{r} h(r\cos 2\pi\theta, r\sin 2\pi\theta, r\bar{\lambda}).$$

This special expression is not unexpected, taking into account the presence of the invariant foliation $\{r\bar{\lambda} = \lambda_0\}$, leading to the relation $\dot{\bar{\lambda}}/\bar{\lambda} = -\dot{r}/r$.

Looking at the first return map to the section $\{\theta = 0\}$ along $\{r = 0, \bar{\lambda} = 0\}$, that we write as $(\bar{\lambda}, r) \overset{P}{\mapsto} (\Lambda, R)$, we see that it is infinitely tangent to the time 1 map of the flow of

$$\begin{cases} \dot{r} = r^2(\bar{\lambda} + r + r^3 g(r^2, r\bar{\lambda})) \\ \dot{\bar{\lambda}} = -\bar{\lambda} r(\bar{\lambda} + r + r^3 g(r^2, r\bar{\lambda})) \ . \end{cases}$$

Hence

$$\begin{aligned} R &= r + r^2\bar{\lambda} + r^3(1 + O(r)) \\ &= r[1 + r\bar{\lambda} + r^2(1 + O(r))] \ . \end{aligned}$$

The Λ-component will give no further information because of the relation

$$\Lambda R = \bar{\lambda} r \ .$$

Fixed points are given by $\{r = 0\}$ and, for $r \neq 0$, by

$$\bar{\lambda} + r(1 + O(r)) = 0 \ .$$

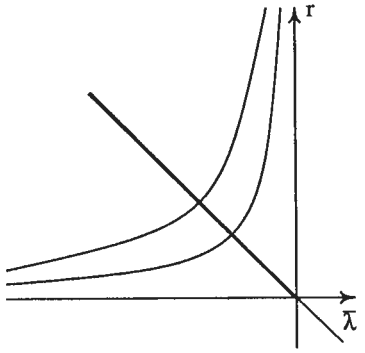

Figure 40 : Line of fixed points of P in $(r, \bar{\lambda})$-space

The line L is transversely cutting the regular leaves of the foliation $\{r\bar{\lambda} = \lambda\}$, and for $\lambda < 0$, there is exactly one hyperbolic fixed point on each leaf. The complete picture (both rescaling charts together) is then (for the (+)-case) :

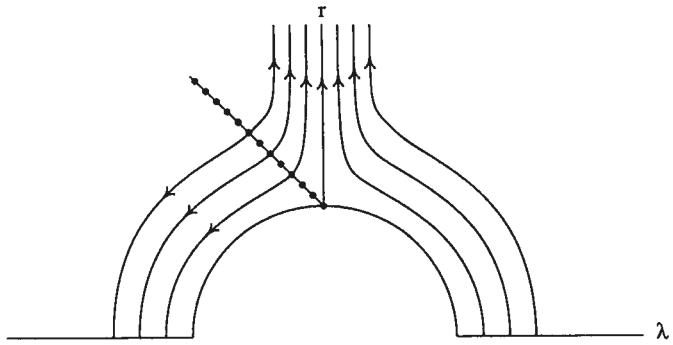

Figure 41 : Line of fixed points of P in the total blow-up space

In the original parameters (r, λ) we hence obtain the picture from Figure 42, that looks very familiar indeed.

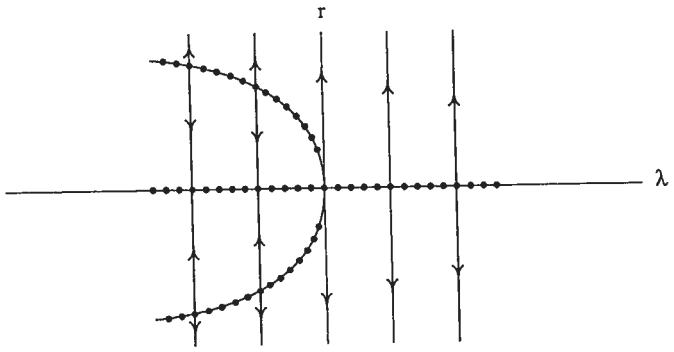

Figure 42 : Line of fixed points of P in (r, λ)-space

Remark In studying the Andronov-Hopf bifurcation, we can also use the quasi-homogeneous blow-up of the family given by

$$(x, y, \lambda) = (r\bar{x}, r\bar{y}, r^2\bar{\lambda}) \ .$$

The vector field $X = X_\lambda$ is then reduced to a vector field $\tilde{X}$ where the unique limit cycle has to be studied by "family rescaling" while the "phase directional rescaling" shows no fixed points at all for $r > 0$.

Appendix 3 Quadratic models for generic 3-parameter unfoldings of nilpotent singularities of codimension 3

As has been proved in [DF] with the help of normal form calculations, there exist 3-parameter families of quadratic vector field in the plane that (locally) represent generic unfoldings of the nilpotent cusp, saddle and elliptic point of codimension 3. This is not possible for the focus since such a singularity can not occur for quadratic vector fields. For the sake of completeness we give here an example for each case.

(i) **Cusp case**

$$X_{a,b,c} : \begin{cases} \dot{x} &= a\,x/3 + (5+7a)y/5 + (30+17a)x^2/30 \\ &\quad +(15b - 206a - 90)xy/45 + (14(b-a) - 5)y^2/10 \\ \dot{y} &= a + (5a+3b)y/3 + (5+6a+5b)x^2/5 \\ &\quad +(5c - 14a - 10)xy/5 + (15b - 25a)y^2/18 \end{cases}$$

(ii) **Saddle case**

$$S_{(a,b,c)} : \begin{cases} \dot{x} = y + x^2 - 2xy \\ \dot{y} = a + bx + cy + (b+c)x^2 - xy \end{cases}$$

(iii) **Elliptic case**

$$E_{(a,b,c)} : \begin{cases} \dot{x} = y + x^2/2 + 2xy \\ \dot{y} = a + bx + cy + (c-b)x^2/2 + 2xy \end{cases}$$

References

[ALGM] Andronov, A., Leontonich, E., Gordon, I., Maier, A., *Theory of Bifurcations of Dynamical Systems on a Plane*, Israel Program for Scientific Translations, Jerusalem 1971.

[B] Bogdanov, R.I., Versal deformation of a singularity of a vector field on the plane in the case of zero eigenvalues, *Seminar Petrovski* 1976 (Russian), *Selecta Math. Soviet.* **1** (1981), 389–421 (English).

[BCD] Benoit, E., Callot, J.L., Diener, F., Diener, M., Chasse au canard, *Collect. Math.* **31-32 (1-3)** (1981), 37–119.

[Bo] Bonckaert, P., Partially hyperbolic fixed points with constraints, preprint.

[Bro] Brocker, Th., Differentiable germs and catastrophes, London Math. Soc. Lecture Note Ser. **17**, 1975.

[BM] Brunella, M., Miari, M., Topological equivalence of a plane vector field with its principal part defined through Newton polyhedra, *J. Differential Equations* **85** (1990), 338–366.

[Br] Bruno, A.D., *Local Methods in Non-linear Differential Equations*, Springer Ser. Soviet Math., Springer-Verlag, Berlin-Heidelberg-New York 1989.

[CD] Chicone, C., Dumortier, F., Finiteness for critical periods of planar analytic vector fields, in: *Nonlinear Analysis: Theory, Methods and Applications*, 1993.

[C1] Coppel, W.A., A survey of quadratic systems, *J. Differential Equations* **2** (1966), 293–304.

[C2] Coppel, W.A., Some quadratic systems with as most one limit cycle, in: *Dynamics Reported Vol. 2*, Dynam. Report. Ser. Dynam. Syst. Appl. **2**, Wiley, Chichester 1989, 61–68.

[D] Dumortier, F., *Singularities of Vector Fields*, Monograf. Mat. **32**, Inst. Mat. Pura Apl., Rio de Janeiro, 1978.

[D1] Dumortier, F., Singularities of vector fields on the plane, *J. Differential Equations* **23** (1977), 53–106.

[D2] Dumortier, F., Local study of planar vector fields: singularities and their unfoldings, in: *Structures in Dynamics, Finite Dimensional Deterministic Studies* (H.W. Broer et al., eds.), Stud. Math. Phys. **2**, North-Holland, Amsterdam 1991, 161–241.

[DF] Dumortier, F., Fiddelaers, P., Quadratic models for generic local 3-parameter bifurcations on the plane, *Trans. Amer. Math. Soc.* **326** (1991), 101–126.

[DRc] Dumortier, F., Rousseau, C., Cubic Liénard equations with linear damping, *Nonlinearity* **3** (1990), 1015–1039.

[DR1] Dumortier, F., Roussarie, R., On the saddle loop bifurcation, in: *Bifurcations of Planar Vector Fields* (J.-P. Françoise and R. Roussarie, eds.), Lecture Notes in Math. **1455**, Springer-Verlag, Berlin-Heidelberg-New York 1990, 44–73.

[DR2] Dumortier, F., Roussarie, R., Tracking limit cycles escaping from rescaling domains, in: *Proc. Intern. Conf. Dynam. Systems and Related Topics*, Adv. Ser. Dynam. Syst. **9**, World Scientific, Singapore 1991, 80–99.

[DR3] Dumortier, F., Roussarie, R., Canard cycles and center manifolds, preprint.

[DRS1] Dumortier, F., Roussarie, R., Sotomayor, J., Generic 3-parameter families of vector fields on the plane, unfolding a singularity with nilpotent linear part. The cusp case, *Ergodic Theory Dynamical Systems* **7** (1987), 375–413.

[DRS2] Dumortier, F., Roussarie, R., Sotomayor, J., Generic 3-parameter families of planar vector fields, unfoldings of saddle, focus and elliptic singularities with nilpotent linear parts, in: *Bifurcations of Planar Vector Fields: Nilpotent Singularities and Abelian Integrals* (F. Dumortier et al., eds.), Lecture Notes in Math. **1480**, Springer-Verlag, Berlin-Heidelberg-New York 1991, 1–164.

[GH] Guckenheimer, J., Holmes, P., *Non-linear Oscillations, Dynamical Systems and Bifurcations of Vector Fields*, Appl. Math. Sci. **42**, Springer-Verlag, Berlin-Heidelberg-New York 1983.

[H] Hirsch, M.H., *Differential Topology*, Graduate Texts in Math. **33**, Springer-Verlag, Berlin-Heidelberg-New York 1976.

[L] Lyapunov, A.M., *Stability of Motion*, Math. Sci. Engrg. **30**, Academic Press, London-New York 1966.

[P] Perko, L., Rotated vector field and the global behavior of limit cycles for a class of quadratic systems in the plane, *J. Differential Equations* **18** (1975), 63–86.

[R] Roussarie, R., Techniques in the theory of local bifurcations: cyclicity and desingularization, this volume.

[T1] Takens, F., Singularities of vector fields, *Inst. Hautes Études Sci. Publ. Math.* **43** (1974), 48–100.

[T2] Takens, F., Partially hyperbolic fixed points, *Topology* **10** (1971), 133–147.

[T3] Takens, F., Forced oscillations and bifurcation, in: *Applications of Global Analysis I*, Comm. Math. Inst. Univ. Utrecht **3** (1974), 1–59.

[V] Vanderbauwhede, A., Center manifolds, normal forms and elementary bifurcations, in: *Dynamics Reported Vol. 2*, Dynam. Report. Ser. Dynam. Syst. Appl. **2**, Wiley, Chichester 1989, 89–169.

[Z] Żołądek, H., Abelian integrals in unfoldings of codimension 3 singular planar vector fields, in: *Bifurcations of Planar Vector Fields: Nilpotent Singularities and Abelian Integrals* (F. Dumortier et al., eds.), Lecture Notes in Math. **1480**, Springer-Verlag, Berlin-Heidelberg-New York 1991, 165–224.